



## Article

# Examining the Effects of Soil and Water Conservation Measures on Patterns and Magnitudes of Vegetation Cover Change in a Subtropical Region Using Time Series Landsat Imagery

Xiaoyu Sun <sup>1,2</sup>, Guiying Li <sup>1,2</sup> , Qinquan Wu <sup>3</sup>, Dengqiu Li <sup>1,2</sup> and Dengsheng Lu <sup>1,2,\*</sup>

<sup>1</sup> Key Laboratory for Humid Subtropical Eco-Geographical Processes of the Ministry of Education, Fujian Normal University, Fuzhou 350117, China; qsx20211151@student.fjnu.edu.cn (X.S.); liguiying@fjnu.edu.cn (G.L.); lidengqiu@fjnu.edu.cn (D.L.)

<sup>2</sup> Institute of Geography, Fujian Normal University, Fuzhou 350117, China

<sup>3</sup> Fujian Soil and Water Conservation Experimental Station, Fuzhou 350003, China; wuqq1227@126.com

\* Correspondence: ludengsheng@fjnu.edu.cn

**Abstract:** Soil and water erosion has long been regarded as a serious environmental problem in the world. Thus, research on reducing soil erosion has received continuous attention. Different conservation measures such as restoring low-function forests, closing hillsides for afforestation, planting trees and grass, and constructing terraces on slope land have been implemented for controlling soil erosion problems and promoting vegetation cover change. One important task is to understand the effects of different conservation measures on reducing water and soil erosion problems. However, directly conducting the evaluation of soil erosion reduction is difficult. One solution is to evaluate the patterns and magnitudes of vegetation cover change due to implementing these measures. Therefore, this research selected Changting County, Fujian Province as a case study to examine the effects of implementing conservation measures on vegetation cover change based on time series Landsat images and field survey data. Landsat images between 1986 and 2021 were used to produce time series vegetation cover data using the Google Earth Engine. Sentinel-2 images acquired in 2021 and Landsat images in 2010 were separately used to develop land cover maps using the random forest method. The spatial distribution of different conservation measures was linked to annual vegetation cover and land cover change data to examine the effects on the change in vegetation cover. The results showed a significant reduction in bare lands and increase in pine forests. The vegetation coverage increased from 42% in 1986 to 79% in 2021 in the conservation region compared with an increase from 73% to 87% in the non-conservation region during the same period. Of the different conservation measures, the change magnitude was 0.44 for restoring low-function forests and closing hillsides for afforestation and 0.65 for multiple control measures. This research provides new insights in terms of understanding the effects of taking proper measures for reducing soil and water erosion problems and provides scientific results for decisionmaking for soil erosion controls. The strategy and method used in this research are valuable for other regions in understanding the roles of different conservation measures on vegetation cover change and soil erosion reduction through employing remote sensing technologies.

**Keywords:** soil and water conservation measures; vegetation cover; patterns and magnitudes; Landsat time series; Changting County



**Citation:** Sun, X.; Li, G.; Wu, Q.; Li, D.; Lu, D. Examining the Effects of Soil and Water Conservation Measures on Patterns and Magnitudes of Vegetation Cover Change in a Subtropical Region Using Time Series Landsat Imagery. *Remote Sens.* **2024**, *16*, 714. <https://doi.org/10.3390/rs16040714>

Academic Editor: Dino Ienco

Received: 8 December 2023

Revised: 18 January 2024

Accepted: 17 February 2024

Published: 18 February 2024



**Copyright:** © 2024 by the authors. Licensee MDPI, Basel, Switzerland. This article is an open access article distributed under the terms and conditions of the Creative Commons Attribution (CC BY) license (<https://creativecommons.org/licenses/by/4.0/>).

## 1. Introduction

Water and soil erosion has long been regarded as a serious environmental problem in the world, and research on reducing erosion has received substantial attention for decades [1–3]. One consequence of soil erosion is the loss of topsoil, which is a fundamental resource for food production and water conservation [4–7]. Because of soil erosion, the remaining soils may become poor in soil structure and fertility, as well as in water and

nutrient holding ability, threatening the sustainability of the land [4,8]. The erosive soils may further result in increased sediments in rivers and reservoirs and deteriorated water quality [9]. Therefore, great efforts have been undertaken to reduce soil erosion problems through various conservation measures, such as engineering projects (e.g., terracing), tree or grass planting, and closing hillsides for afforestation [10–12].

Direct evaluation of soil erosion reduction is challenging; however, implementing different conservation measures for controlling water and soil erosion will alter the land surface features, particularly vegetation coverage [13]. Thus, we can examine how vegetation cover changes over time to better understand the effects of implementing conservation measures on reducing soil erosion problems [14]. The traditional methods for monitoring soil erosion and assessing the effects of controlling measures are based on field survey through runoff plot experiments [15] and sediment collectors [16]. Although field measurements provide the most reliable data regarding soil loss, they cannot provide erosion observations at spatial and temporal scales due to their time-consuming and labor-intensive nature. The complexity of land surface features and terrain conditions also makes it difficult to produce the spatial distribution of soil erosion based on a limited number of field measurements. The same problem exists for the field measurement of vegetation sample plots.

Another possible method is the use of soil erosion models to estimate the erosion amount based on the factors affecting soil erosion. Such factors include soil properties, topography (slope steepness and slope length), rainfall (amount and intensity), vegetation cover, and human intervention practices [17,18]. However, the different quality and characteristics of data sources (e.g., soil, topography, climate data, and remotely sensed data) make estimation highly uncertain in mountainous regions using the erosion models, thus resulting in difficulty to quantitatively assess whether the land is degraded or restored [19]. The possible solution may be the use of remote sensing technologies, especially satellites, because of the ability to capture data coverage in large areas and repetitive acquisition. The advantages of remote sensing technology over traditional methods make it the major source for obtaining Earth surface features such as land cover types and vegetation change at low cost. Because of the close relationship between land surface features and soil erosion, remote sensing data become an indispensable means for monitoring soil erosion and evaluating the effectiveness of soil erosion controls on ecosystem functions [20,21].

Vegetation cover is one of the most important factors influencing soil erosion, especially in mountainous regions [21,22]. The presence of vegetation cover can reduce and prevent splash erosion by intercepting rain, increased infiltration, and slow surface runoff, thus significantly reducing sheet erosion [20]. The vegetation root system anchors and reinforces soil and stabilizes slopes. Generally speaking, the more vegetative cover, the lower the risk of soil erosion. Therefore, increasing vegetation cover is considered an effective measure for controlling soil erosion, and vegetation restoration level is an important indicator to evaluate the effectiveness of a conservation measure in controlling soil and water erosion [22–24]. Research has shown that, in mountainous areas, restoring vegetation cover to more than 78% can significantly reduce soil erosion caused by water [22].

Vegetation cover can be estimated by optical remote sensing data such as MODIS, Landsat, and Sentinel-2 images [25–27]. Although MODIS data have the advantage for monitoring vegetation cover dynamics with high temporal resolution, the coarse spatial resolution limits vegetation cover extraction at a fine scale. In contrast, Sentinel-2 data can provide fine-resolution vegetation cover data [28], but the short historical record is not able to provide vegetation cover dynamics in the long term. Because of the availability of long-term data archives at no cost [29,30], Landsat becomes the most common data source for the extraction of vegetation coverage. In general, vegetation distribution is often developed from Landsat imagery using classification algorithms such as maximum likelihood and machine learning [31–33]. These methods usually provide pixel-level vegetation coverage. Considering the complexity of land cover types, one solution is to develop fractional vegetation cover using spectral mixture analysis [34]. However, this method takes time to unmix multispectral images into fractional images, whose fractional values are influenced

by external conditions such as atmospheric conditions; thus, the fractional images have uncertainty, and time series fractional vegetation images may be ineffective for the detection of vegetation cover change. Lu et al. (2007) proposed a surface cover index (SCI) based on fractional images that were derived from the multispectral image for examining land degradation in the Amazon basin [35]. In addition to the fractional images, vegetation cover that can be extracted from the normalized difference vegetation index (NDVI) can also be used as an index to explore the land degradation or restoration [22].

Contrary to prior studies that solely concentrated on the effect of vegetation cover, vegetation components, or vegetation patterns on runoff and soil erosion [22–24,36], the current investigation strives to explore the effects of different conservation measures for water and soil loss controls on patterns and magnitudes of vegetation cover change. The research selects a subtropical region—Changting County, Fujian Province—as a case study to examine how vegetation cover changes respond to different conservation measures for better understanding the impact of diverse interventions on the mitigation of soil erosion. Changting was listed as one of three major soil erosion control experimental areas in China (the other two were Chang’an in Shaanxi Province and Tianshui in Gansu Province) as early as the 1940s. Soil erosion in Changting is characterized by a large extent, high severity, great risk, and a long history of controlling. It is the most serious and representative area of red soil erosion in southern China. This research will be valuable for making proper decisions to take measures to reduce soil erosion problems in similar climates and geographical regions. Because vegetation restoration is widely known as an effective measure of ecological construction and soil erosion control across a variety of environmental conditions [37,38] and Landsat time series data are available globally, the methods used in this research may be applicable in different climates and terrains in tropical and subtropical regions.

## 2. Study Area

Changting County is located in the mountainous area of western Fujian Province, China (Figure 1). It consists of 18 townships, covering a total area of 3104 km<sup>2</sup>. The terrain of this county is complex, with mainly low hills (about 71.1%) and uplands, and has the common characteristics of ‘eight mountains, one water and one field’ in Fujian Province. The climate in Changting belongs to subtropical monsoon, with hot and humid summers and mild and dry winters. The average annual temperature is 18.3 °C, with January averaging 12.5 °C and July averaging 27.8 °C. Extreme temperatures range from 39.7 °C to −3.5 °C. The annual average precipitation is 1730 mm, with varying occurrences of typhoon-induced heavy rains ranging between 200 and 350 mm [39]. There are rich river systems in the county, including the Han, Min, Gan, and Ting Rivers, of which the Ting River forms the largest watershed.

The soil in Changting County is primarily red soil developed by granite, which is easily weathered in high-temperature and humid subtropical areas [40]. Historically, it was covered by dense vegetation with light soil erosion [41]. However, the primary evergreen broadleaf forests were almost destroyed due to long-term human destruction (e.g., multiple wars during the mid-17th to the early 20th century, disputes over mountain and forest ownerships, and feudal clan conflicts throughout dynasties), or replaced by secondary forest vegetation, commonly coniferous forests (mainly *Pinus massoniana*), secondary evergreen broadleaf forests, shrubs, and others, causing significant reductions in vegetation coverage [42,43]. The ecological condition was worsened due to anthropogenic activities such as cutting down trees for fuel and cultivating on steep slopes. Those human interventions and natural factors, such as concentrated intense rainfall, frequent tectonic movement, high soil erodibility, and less vegetation cover, have made Changting County a fragile ecological environment, becoming one of the most typical soil erosion cases in southern China’s hilly red soil regions [19,44]. Thus, Changting County was once notorious for ‘flaming mountains’ due to red soil exposure [45].

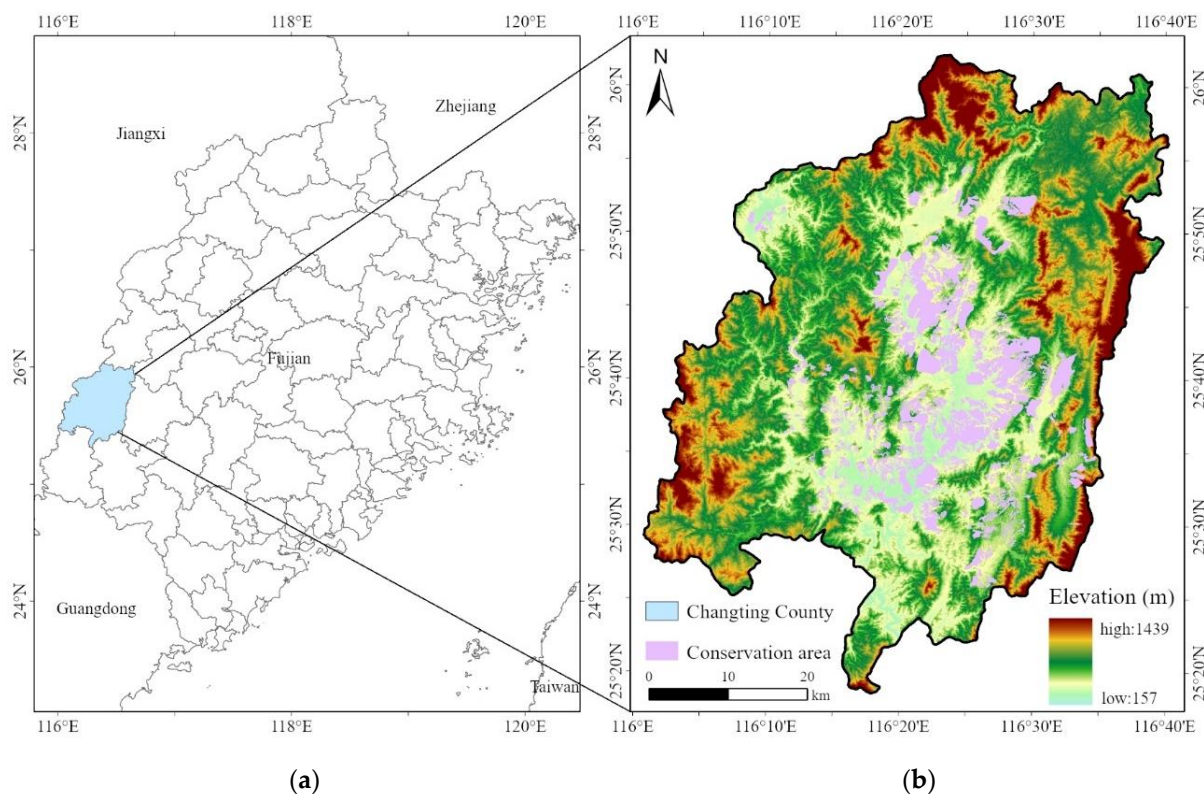


**Figure 1.** The location of study area—Changting County, Fujian Province, China ((a)—County boundaries of Fujian Province; (b)—elevation map of Changting County, overlaid by the conservation area).

Water and soil erosion in Changting have long been problems faced by the local government and residents. A survey conducted in 1985 by the local government found that about 100,000 hectares of land, accounting for 31.5% of the county's area, were subject to water and soil erosion, involving seven townships, including Hetian, Sanzhou, and Cewu. The annual soil loss reached 5000–12,000 tons/km<sup>2</sup>, and the vegetation cover rate was as low as only 5% [46]. In 1983, efforts to control and curb water and soil erosion were initiated by the Fujian provincial government, and Changting was listed as a key trial area for such efforts. Joint research on water and soil conservation was carried out by the local government, universities, and institutes. Since then, the provincial government has increased its financial and technological support for the county to harness soil erosion and water loss. Adhering to ecological priorities and green development in building an ecological civilization in China, the integration of biological and engineering measures was implemented for vegetation restoration to alleviate water and soil erosion. After decades of efforts, Changting County has undergone a complete transformation from “flaming (barren) mountains” to “lushly green mountains”. As of 2021, the forest cover rate in Changting reached 80%, while the soil erosion area shrank to 210 km<sup>2</sup>, accounting for only 6.78% of the county area. Changting has achieved a worldwide reputation for its efforts and success in controlling water loss and soil erosion, and ‘Changting’s experience’ was shared at the United Nations Biodiversity Conference (COP15), providing a Chinese approach to environmental protection to the world [47].

### 3. Datasets and Methods

In order to examine the effect of soil and water conservation measures on patterns and magnitudes of vegetation cover change in Changting County, we designed the following scheme (Figure 2) showing the major steps of processes, including data collection (e.g., field survey data, historical records of conservation measures, and remotely sensed data), land cover map creation using Sentinel-2 imagery in 2021 and Landsat imagery in 2010,

separately, land cover change detection using the post-classification comparison method based on classified results between 2021 and 2010, annual fractional vegetation cover (FVC) extraction using time series Landsat images between 1986 and 2021, and analysis of FVC changes in relation to land cover changes as well as the conservation measures. Considering the importance of producing accurate land cover classification results, Sentinel-2, due to its higher spatial resolution and more spectral bands than Landsat imagery, was selected for land cover classification in 2021 using random forest algorithm. However, only Landsat imagery in 2010 was available for land cover classification. Before conducting land cover change detection, the classified image with 10 m spatial resolution in 2021 was resampled to 30 m spatial resolution using the majority function, the same cell size as the 2010 classified image.

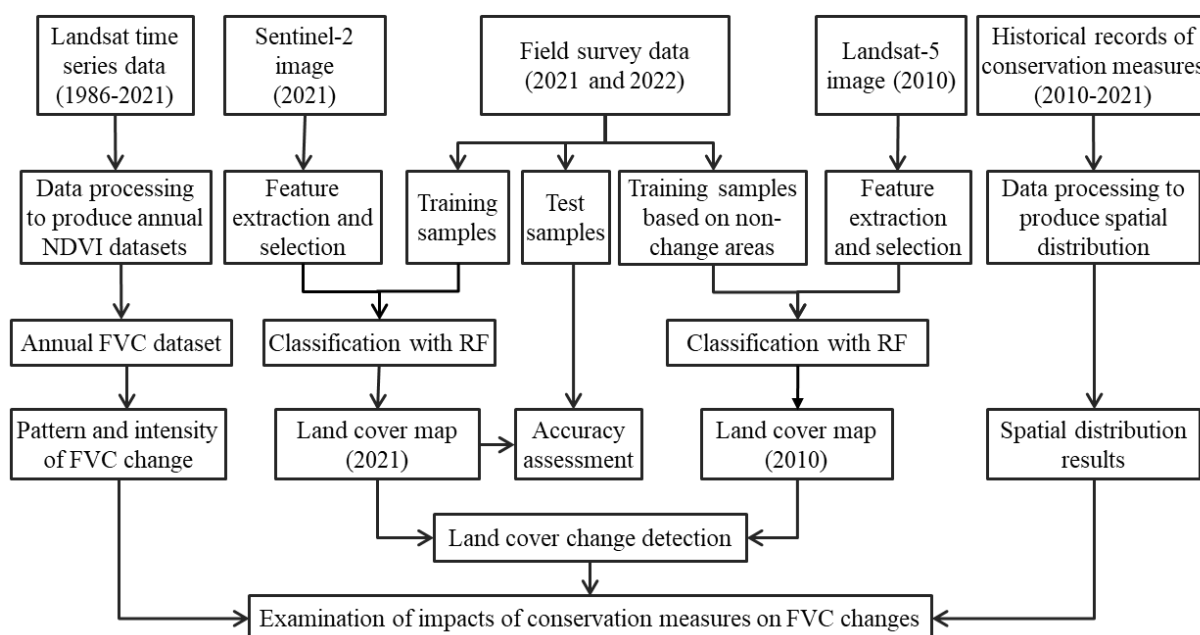


**Figure 2.** The framework of the study (note: NDVI—normalized difference vegetation index; FVC—fractional vegetation cover; RF—random forest).

### 3.1. Data Collection and Preprocessing

Landsat time series images from 1986 to 2021, Sentinel-2 multispectral data in 2021, field survey samples of different land cover types, historical records of implementing conservation measures, and ancillary data were collected and preprocessed.

#### 3.1.1. Collection of Field Survey Data for Land Cover Mapping

Field surveys of different land cover types were conducted in August 2021 and January 2022. The information about land cover type, topography, and vegetation status (e.g., age and tree species) was recorded. The collected samples of land cover types were allocated on the Sentinel-2 image and scrutinized to ensure their validity. Moreover, 60% of samples were randomly selected and used as a training set for image classification, and the rest were used as a validation set for accuracy assessment. According to the field survey, there are some fruit lands, such as Chinese bayberry and orange; however, their areas are tiny, and fruit tree crowns are small; thus, they are hardly differentiated from bare bands on satellite image acquired in the winter season. Therefore, fruit lands were not considered in the classification. The land cover types included Masson pine, Chinese fir, broadleaf forest (such as chestnut forest and mixed broadleaf forest), bamboo forest, farmland, bare land, impervious surface area (ISA), and water body.

### 3.1.2. Collection of Data Related to Water and Soil Conservation Measures

Various conservation measures for controlling soil erosion have been practiced in Changting County since the 1980s, depending on local biophysical and socio-economic conditions. These measures can be categorized into six types: restoring low-function forests, closing hillsides for afforestation, planting fruit trees, planting trees and grass, constructing terraces on slope land, and multiple control measures (due to failure in previous measures). Table 1 presents the detailed descriptions of six conservation measures. Because the spatial information of conservation measures in the early years was not available, we only collected the conservation records from 2010 to 2021, containing conservation measures, locations, and implementation dates, from Changting's Bureau of Soil and Water Conservancy. These data were organized into polygon vectors within GIS platform (Figure 3). The regions where conservation measures were implemented are called the conservation zones, while the regions outside of the conservation zones are named non-conservation zones. In addition, we selected three typical areas (barren land, contrast land, and non-erosion area) within the non-conservation zones according to vegetation coverage conditions for comparison purposes later. Their explanations can also be found in Table 1.

**Table 1.** Brief descriptions of different conservation measures used in this study area.

Conservation Measures	Descriptions	Area (ha)
Restoring low-function forests	Implementing forest management, including replacement and transformation, replanting, and tending, to improve the forest stand structure, increase the production potential of forestlands, and to enhance forest quality and benefits.	1347
Closing hillsides for afforestation	Taking advantage of the regeneration capacity of forests and closing mountainous areas to promote forest regeneration and growth by prohibiting interference from external factors, such as people and livestock on forestlands.	24,711
Planting trees and grass	Planting suitable trees and grass to increase vegetation coverage, prevent soil erosion, and improve land productivity.	4625
Planting fruit trees	Planting fruit trees of high cash value for both ecological and economic benefits.	26
Constructing terraces on slope land	Transforming slope land that is prone to water, soil, and fertilizer losses into terraces for convenient farming.	131
Multiple measures	Continuously implementing different conservation measures after the failure of the previous efforts.	1457
Barren land	Without vegetation cover, experienced soil erosion problems without implementing any conservation measures.	
Contrast land	With little vegetation cover, experienced soil erosion problems without implementing any conservation measures.	278,262
Non-erosion	High vegetation cover without soil erosion problems.	

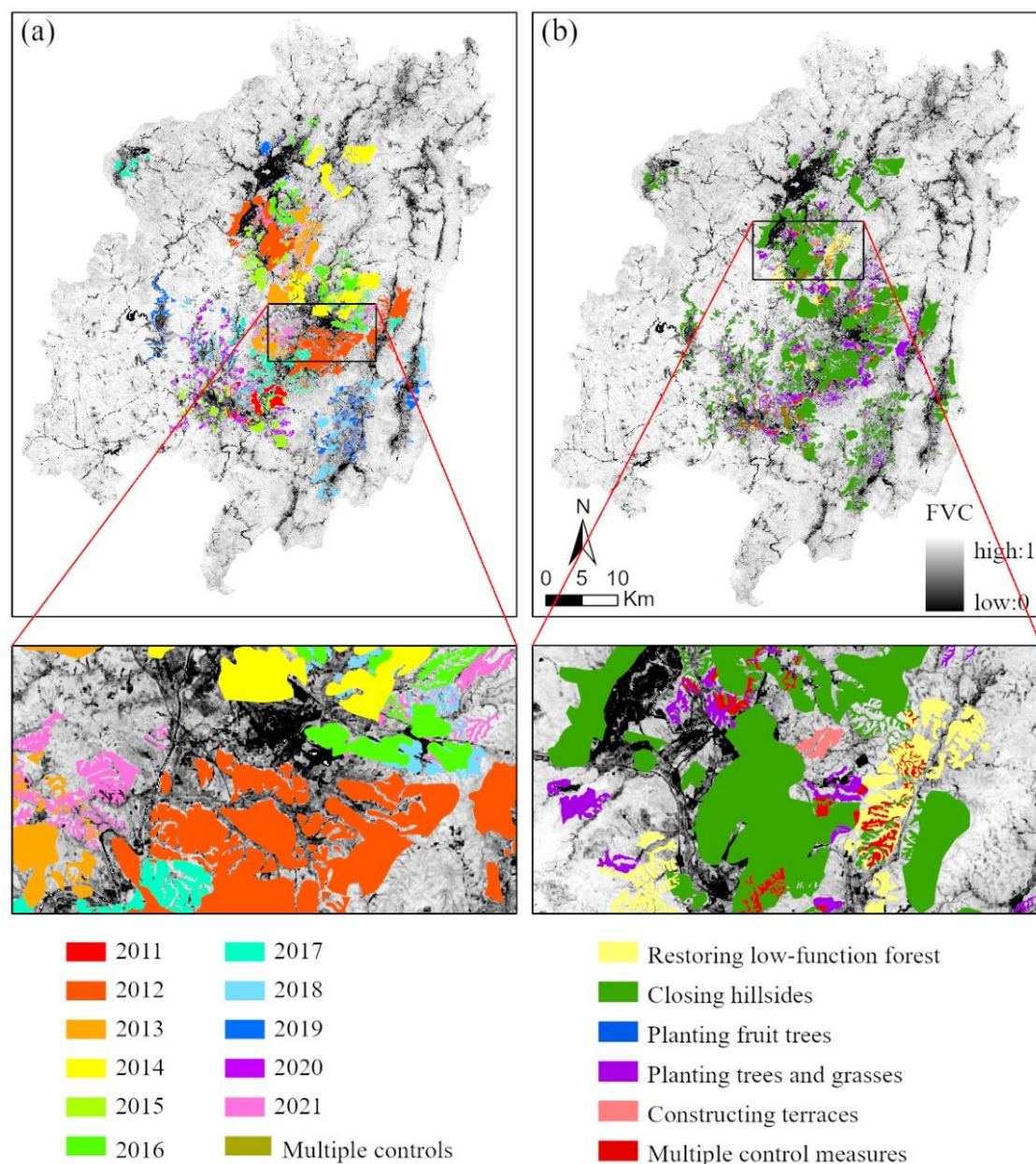


**Figure 3.** Conservation dates and measures implemented in Changting County overlaid on fractional vegetation cover (FVC) in 2021 ((a)—the years of conservation measures implemented between 2010 and 2021; (b)—the practiced conservation measures).

### 3.1.3. Collection and Preprocessing of Remotely Sensed Data

Landsat 5 Thematic Mapper (TM) and Landsat 8 Operational Land Imager (OLI) Land Surface Reflectance (LSR) time series images covering Changting County from 1986 to 2021 were obtained with the GEE platform (<https://earthengine.google.com> (accessed on 1 March 2023)). Due to the failure of the Landsat 7 Enhanced Thematic Mapper Plus (ETM+) scan line corrector (SLC), the images collected after 31 May 2003 exhibit wedge-shaped scan-to-scan gaps; thus, Landsat 7 ETM+ images were not included in this research. Because no Landsat images are available in 2012, to avoid data gap in the time series, we used the averages of 2011 and 2013 to replace the 2012 image.

The LSR data were atmospherically corrected using LEDAPS (Landsat Ecosystem Disturbance Adaptive Processing System) (for Landsat 5 TM) [48] and LaSRC (Landsat 8 Collection 1 Land Surface Reflectance Code) (for Landsat 8 OLI) [49] algorithms. The

images acquired between April and October with cloud coverage of less than 50% were collected. Based on the associated QA (quality assessment), the pixels labeled with low quality, such as clouds, snow, and shadows, were removed, and then NDVI for each selected image was calculated. The median value of NDVI during a year was extracted as a yearly NDVI composite, and then the yearly NDVI from 1986 to 2021 formed the time series NDVI datasets that were used to calculate annual FVC later.

Since 2010, Changting County has started to implement intensive management for soil erosion control, resulting in tremendous land cover changes. Thus, Landsat-5 TM multispectral data dated 14 January 2010 and Sentinel-2 Level-2A multispectral product with spatial resolution of 10 m dated 31 January 2021 were obtained from GEE. These images were geometrically corrected with a registration error of less than 0.5 pixels. Then, the topographic correction was conducted based on the Shuttle Radar Topography Mission (SRTM) DEM data using SCS + C method [50], which was proven to be the most appropriate in forested terrain. The corrected images were used to develop land cover maps in 2010 and 2021.

#### 3.1.4. Ancillary Data

The ancillary data include the Changting County boundary and the digital elevation model (DEM). Changting County boundary shapefile was extracted from China administrative divisions at county level, which was downloaded from the National Catalogue Service for Geographic Information (<https://www.webmap.cn> (accessed on 15 November 2022)). The boundary file was used to delineate the study area through clipping all other datasets. The SRTM DEM data with a resolution of 30 m were downloaded from the USGS website (<https://lpdaac.usgs.gov/> (accessed on 15 November 2022)), which were used in topographic correction of Landsat and Sentinel-2 images and for deriving topographic features (elevation, slope, and aspect) as additional inputs in image classification.

### 3.2. Methods

#### 3.2.1. Land Cover Classification and Change Detection

With land cover samples collected in 2021–2022 as ground truth data, the land cover classification was first implemented using the 2021 Sentinel-2 images due to their higher spatial resolution and more spectral bands than Landsat imagery. The potential features for classification included 10 spectral bands, 3 vegetation indices (NDVI, Normalized Difference Wetness Index (NDWI), and Enhanced Vegetation Index (EVI)), 320 textures derived using the Gray Level Co-occurrence Matrix (GLCM) based on 10 spectral bands with window sizes of  $3 \times 3$ ,  $5 \times 5$ ,  $7 \times 7$ , and  $9 \times 9$ , and 3 topographic features (elevation, slope, and aspect) derived from SRTM DEM. Random forest (RF) was used to provide the importance rankings of these variables. Based on the features' importance rankings and correlations between these features, the most important features were chosen for classification using RF algorithm [51]. The parameters in RF classification were set as 500 for the number of trees, 'square root' for the number of features, and default values for other parameters. The classification result was further processed with a majority filter tool ( $3 \times 3$  pixels) to remove noise.

The development of land cover map for 2010 was more complex due to lack of ground truth data. We took the 2021 land cover map developed from Sentinel-2 images as a reference and collected the land cover samples from it. First, we resampled the land cover classification image of 2021 into 30 m to match the Landsat image. Then, with the aid of the vegetation change trend from the NDVI time series and the resampled land cover map, land cover samples for 2010 were chosen from the areas where there were no significant NDVI changes. Finally, the same classification procedures were applied to the 2010 Landsat 5 TM image for developing a land cover map.

The land cover classification result of 2021 was evaluated using test samples and overall accuracy, producer's accuracy, user's accuracy, and kappa coefficient were calculated from the confusion matrix. Because of a lack of ground truth data in 2010, the

classification accuracy in 2010 was not assessed but was assumed to be similar to the 2021 classification results. The post-classification comparison approach was used to detect land cover change based on the 2010 and 2021 classification results, and a detailed land cover conversion matrix was created. Major land cover change categories, particularly those related to conservation efforts such as the conversion from bare soils to various forest types and croplands, were examined.

The area and percentage of each land cover type within Changting County, the conservation zones, and non-conservation zones in 2010 and 2021 were calculated and compared. The changes in forest types, especially the expansion of various forest types within these zones (entire county, conservation zones, and non-conservation zones), were examined.

### 3.2.2. Extraction of Annual Fractional Vegetation Cover (FVC) from the Time Series Landsat NDVI Images

The dimidiate pixel model is a commonly used linear model for pixel decomposition [52]. It assumes that the spectral response of a pixel is the linear mixture of responses from vegetation and non-vegetation (i.e., bare soil), and the NDVI value of each pixel is the weighted sum of the NDVI values corresponding to pure vegetation and bare soil, while the weight sizes are the areal percentage occupied by two parts within a pixel. Thus, the proportion occupied by the vegetation in each pixel, i.e., the fractional vegetation cover (FVC), can be calculated from NDVI using Equation (1) [53,54]:

$$FVC = \frac{NDVI - NDVI_{soil}}{NDVI_{veg} - NDVI_{soil}} \quad (1)$$

where *FVC* is the fractional vegetation cover within a pixel, *NDVI* is the normalized difference vegetation index of a pixel,  $NDVI_{veg}$  and  $NDVI_{soil}$  are the NDVI values of a pixel with vegetation and bare soil, respectively. In this study, for a given yearly median composite NDVI image, the NDVI value at the 95th percentile was taken as  $NDVI_{veg}$  and NDVI value at the 5th percentile as  $NDVI_{soil}$ . The annual FVC time series images from 1986 to 2021 were calculated using Equation (1). To examine and compare the FVC change trends over time, the average FVC at Changting County, conservation zones, and non-conservation zones for each year were computed.

### 3.2.3. Patterns and Magnitudes of FVC Change

The ‘shape selection forest’ method [55] for fitting nonparametric shape-restricted regression splines to Landsat time series images was used to examine vegetation cover change in this research. For each pixel of a selected spectral band or a vegetation index in Landsat time series, this method can produce a smooth temporal trajectory, representing one of seven possible ‘shapes’ or ‘trend patterns’—flat, decreasing, sudden jump, double jump, vee, inverted vee, and increasing, which reflect the responses of forestland pixels to different disturbances occurring in forested ecosystems. The detailed meanings of these shapes can be found in Moisen et al. [55]. In this study, the FVC time series from 1986 to 2021 were used as the input to ShapeSelectForest package in R software, and the fitting and shape matching methods based on goodness of fit and a penalty were applied to determine the optimal shape to derive the patterns of vegetation changes over time in Changting. According to local FVC characteristics, sudden jump and double jump were combined as jump shape; thus, six shapes were identified, and their change patterns are illustrated in Figure 4.

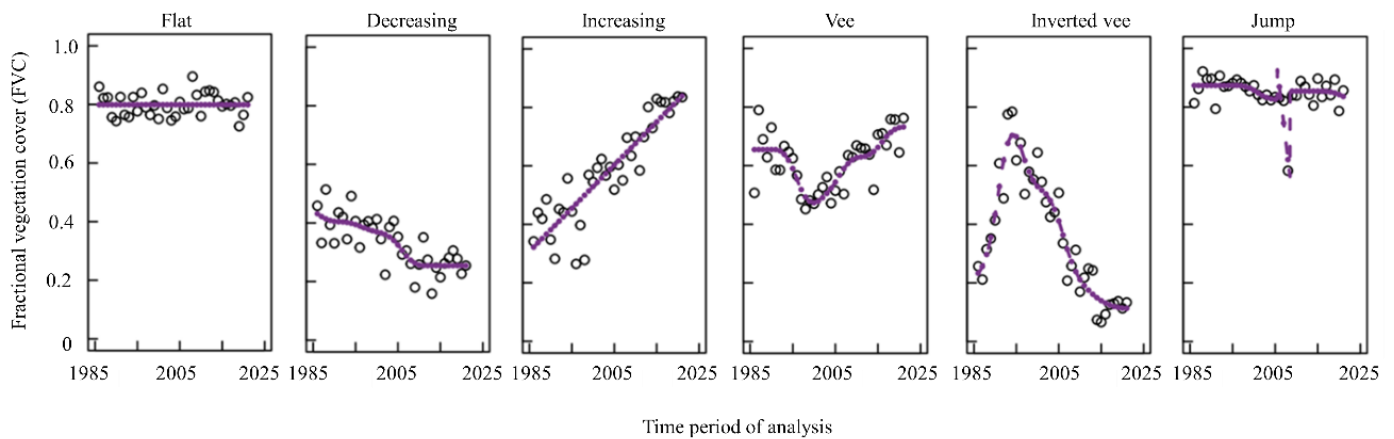


**Figure 4.** Typical shapes of vegetation change patterns.

The output shape parameters from ShapeSelectForest include the onset year of a change, change duration, change magnitude, and others. The change magnitude is defined as

$$Magnitude = \left| \frac{FVC_{start} - FVC_{end}}{FVC_{start}} \right| \quad (2)$$

where magnitude is the change in intensity caused by a disturbance event,  $FVC_{start}$  and  $FVC_{end}$  are FVC values at the start and at the end of the disturbance event, respectively. The change magnitude was classified into five levels: non-change (<0.05), light (0.05–0.15), moderate (0.15–0.30), severe (0.30–0.50), and extreme (>0.50).

The spatial distributions of shapes (change patterns) and change magnitudes in Changting County were generated from ShapeSelectForest. Overall FVC change patterns and magnitudes within Changting County, the conservation zones, and non-conservation zones were analyzed, respectively. Some typical sites were selected in both conservation zones and non-conservation zones in Hetian Township, where the soil erosion problems were very severe. The typical sites in the conservation zones were chosen under different conservation measures, while the ones in non-conservation zones were chosen based on vegetation cover conditions at the beginning of the study period and named as ‘barren land’, ‘contrast land’, and ‘non-erosion land’. Both ‘barren land’ and ‘contrast land’ experienced soil erosion problems, but no conservation measures had been implemented. The difference between them was no vegetation cover at all in ‘barren land’ and sparse vegetation in ‘contrast land’. ‘Non-erosion land’ represents high vegetation cover regions without erosion problems. The FVC change curves over time at those selected typical sites were extracted, and their change patterns were analyzed.

### 3.2.4. Effects of Implementing Conservation Measures on Land Cover Changes

The distribution map of conservation measures was superimposed onto the land cover map of 2021 and the land cover change map between 2010 and 2021. The area of each land cover type under each conservation measure and its areal proportion in the total area of each conservation measure were calculated using Equation (3).

$$FC_{ij} = \frac{Area_{ij}}{Area_i} \quad (3)$$

where  $FC_{ij}$  is the areal percentage of land cover type  $j$  accounted for in the total area of conservation measure  $i$ ,  $Area_{ij}$  is the area of land cover type  $j$  under conservation measure  $i$ ,  $Area_i$  is the total land area in which conservation measure  $i$  was implemented. Because the lands on which the conservation measures of ‘planting fruit trees’ and ‘constructing terraces on slope land’ were implemented accounted for a very small portion and were

mainly coincident with ‘multiple control measures’, they were not included for further analysis.

### 3.2.5. Effects of Implementing Conservation Measures on FVC Changes

To understand the effects of implementing conservation efforts on vegetation recovery, the areas and proportions of FVC change patterns and magnitudes were calculated for the entire county, conservation zones, and non-conservation zones; the composites were compared and analyzed. The distribution map of the conservation measures was superimposed onto the FVC change pattern map and the change magnitude map for calculating the area and areal percentage of each change pattern to the total area of each conservation measure. The minimum, first quartile, median, and third quartile, and the maximum of FVC change magnitude under different conservation measures in conservation zones and non-conservation zones were extracted and used for creating a boxplot showing the differences in change magnitudes among conservation measures. A similar analysis was also conducted based on the distribution of the conservation measures, the distribution of forest types in 2021, and FVC change patterns and magnitude maps.

## 4. Results

### 4.1. Analysis of Land Cover Classification and Change Detection Results

The classification accuracy assessment result for the year 2021 (Table 2) indicates an overall accuracy of 86% and a kappa value of 0.84. Both the user’s and producer’s accuracies for all land cover types are over 75% but vary among land cover types. For example, Masson pine, Chinese fir, and broadleaf forest have lower classification accuracy values than other land cover types. Both Masson pine and Chinese fir are coniferous and have similar spectral responses, making it difficult to differentiate between them. What is more, Masson pine and Chinese fir often grow together with broadleaf species, forming many mixed pixels, which also contributed to the low accuracies of these three forest types. In contrast, bamboo has a higher reflectance in the green band than other land features, resulting in high classification accuracy. In addition, the similar spectral responses between the fallow farmland and bare land regarding the Sentinel-2 data caused their relatively low accuracies.

**Table 2.** Confusion matrix from the classification results based on Sentinel-2 data in 2021.

Land Cover Types	Reference Data									UA (%)	
	Masson Pine	Chinese Fir	Broad-Leaf	Bamboo	Farmland	Bare Land	ISA	Water	Subtotal		
Classification	Masson pine	27	6	3	0	0	0	0	0	36	75.0
	Chinese fir	5	24	3	0	0	0	0	0	32	75.0
	Broadleaf	2	2	24	3	0	0	0	0	31	77.4
	Bamboo	0	0	0	28	0	1	0	0	29	96.6
	Farmland	0	0	0	0	28	2	1	2	33	84.9
	Bare land	0	0	0	1	2	26	0	0	28	92.7
	ISA	0	0	0	0	1	1	30	0	32	93.8
	Water	0	0	0	0	1	0	0	28	29	96.6
Subtotal	34	32	30	31	32	30	31	30	250		
PA (%)	79.4	75.0	80.0	90.3	87.5	86.7	96.8	93.3			

Overall accuracy: 86.0%; kappa: 0.84

Note: ISA represents impervious surface area; UA and PA represent user’s and producer’s accuracy.

A comparison of the land cover maps of 2010 and 2021 indicates that the overall land cover distributions are similar in the two years, with forests being the largest portion, among which Masson pine forests occupied the largest area and were distributed all over the county. Chinese fir forests were concentrated in the east and north of the county; broadleaf forests were mainly distributed in the west, and Moso bamboo forests were scattered in the northwest of the county. The obvious changes on the 2021 map compared to the 2010 map include that a large area of bare land (dark red color) disappeared, while the

Masson pine forests expanded on bare land (Figure 5). A close analysis of the percentages of each land cover type in the two years determined that each land cover type experienced changes to various degrees (Table 3). The area of bare lands shrank by 32,212 ha (from 48,969 ha in 2010 to 16,757 ha in 2021) in the whole county, of which 7274 ha (from 9758 ha in 2010 to 2484 ha in 2021) was in the conservation zones and the rest was in the non-conservation zones. Masson pine forests occupied the largest portion of Changting County. From 2010 to 2021, the area of Masson pine forests increased by 9746 ha (from 136,101 ha in 2010 to 145,847 ha in 2021), of which 6595 ha were located in the conservation zones, particularly in the Hetian basin where soil erosion was severe, making the proportion of Masson pine forests in the conservation zones increase from 45.9% to 66.4%. Chinese fir forests accounted for a small portion, especially in the conservation zones, due to poor site conditions. Their areas expanded from 18,636 ha in 2010 to 27,118 ha in 2021 for the whole county, but most of them were found in non-conservation zones. Broadleaf forests accounted for about one-fourth of the county's area. Overall, their area increased by 3088 ha, but this increase occurred in the non-conservation zones. Bamboo forests accounted for a tiny portion and did not change much from 2010 to 2021, either in the conservation or non-conservation zones. Farmland expanded to a large extent, by 7479 ha, mostly in the non-conservation zones. ISA expanded outward from the original towns and villages; the area increased by 3962 ha, of which about one fourth occurred in the conservation zones and the remaining in the non-conservation zones. Overall, the large increase in Masson pine forests and decrease in bare land in the conservation zones imply that Masson pine, the well-known pioneer tree species for afforestation and reforestation, played an important role in controlling water and soil erosion in the conservation zones as well as in the whole county. Masson pine has strong adaptability and high tolerance to drought and barren soil [56] and is able to grow and regenerate in a harsh environment. Once Masson pine trees take root in soil-eroded areas and enlarge their crowns, they can effectively protect the soil from being washed away by surface runoff, reducing the occurrence of soil erosion.

**Table 3.** The areas (ha) and proportions (%) of land cover types within Changting County, conservation, and non-conservation zones.

Land Cover Types	Statistics in 2010			Statistics in 2021		
	Changting County	Conservation Zones	Non-Conservation Zones	Changting County	Conservation Zones	Non-Conservation Zones
	Area (ha) (%)	Area (ha) (%)	Area (ha) (%)	Area (ha) (%)	Area (ha) (%)	Area (ha) (%)
Masson pine	136,101 (43.8)	14,835 (45.9)	121,266 (43.6)	145,847 (47.0)	21,430 (66.4)	124,416 (44.7)
Chinese fir	18,636 (6.0)	327 (1.0)	18,309 (6.6)	27,118 (8.7)	960 (3.0)	26,158 (9.4)
Broadleaf forest	77,519 (25.0)	4093 (12.7)	73,426 (26.4)	80,607 (26.0)	2796 (8.7)	77,811 (28.0)
Bamboo forest	7271 (2.3)	413 (1.3)	6859 (2.5)	7229 (2.3)	768 (2.4)	6461 (2.3)
Farmland	2408 (0.8)	571 (1.8)	1837 (0.7)	9887 (3.2)	788 (2.4)	9099 (3.3)
Bare land	48,969 (15.8)	9758 (30.2)	39,211 (14.1)	16,757 (5.4)	2484 (7.7)	14,274 (5.1)
Water	3061 (1.0)	327 (1.0)	2734 (1.0)	2558 (0.8)	206 (0.6)	2352 (0.9)
Impervious surface area	16,595 (5.3)	1974 (6.1)	14,621 (5.3)	20,557 (6.6)	2866 (8.9)	17,691 (6.4)
Total	310,560 (100)	32,298 (100)	278,262 (100)	310,560 (100)	32,298 (100)	278,262 (100)

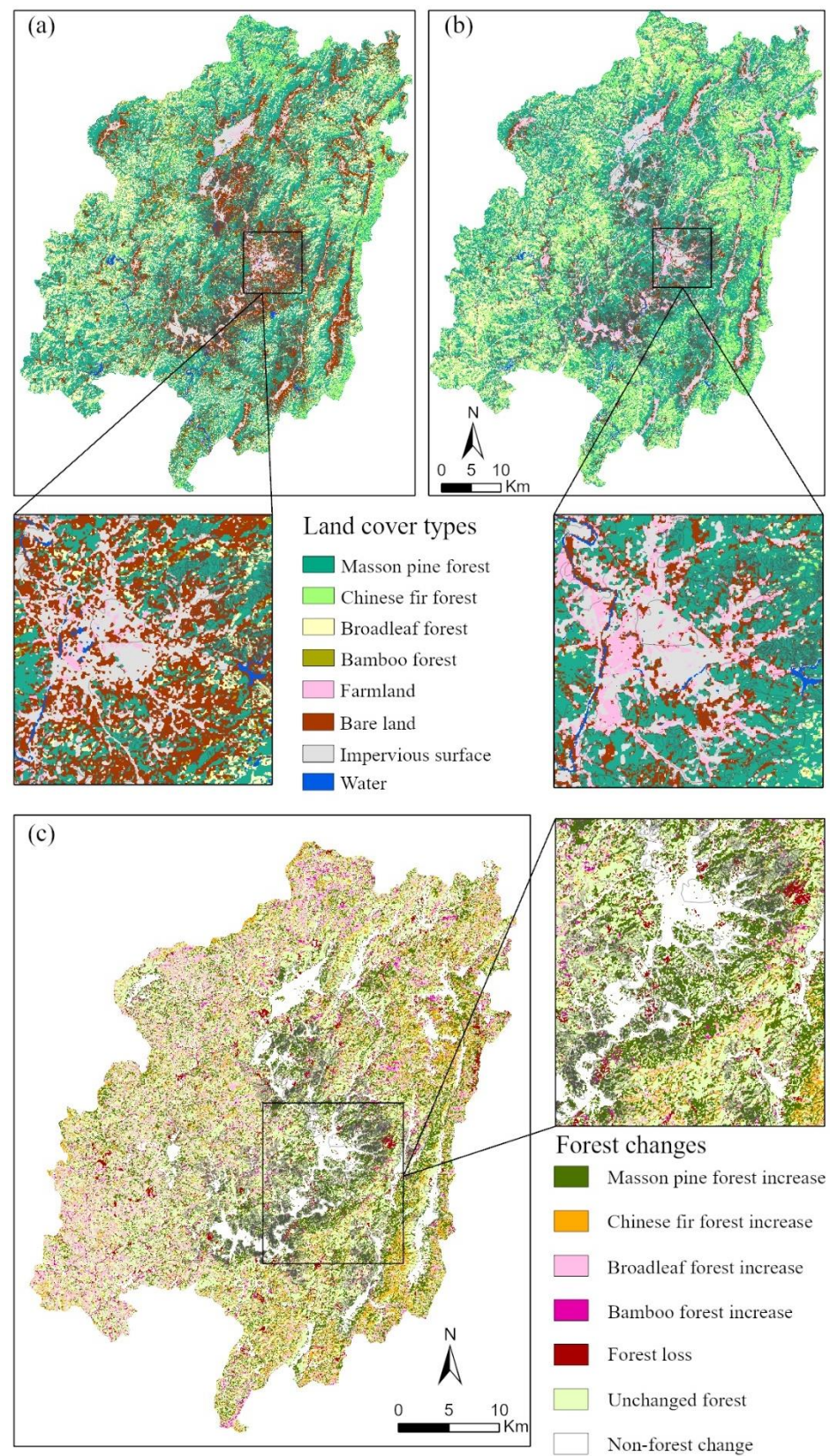


**Figure 5.** Land cover distribution and change detection results ((a)—land cover classification based on Landsat TM image in 2010; (b)—land cover classification based on Sentinel-2 image in 2021; (c)—forest changes from 2010 to 2021; here, ‘increase’ means the conversions from other land cover types to this type, and ‘loss’ means the conversion from forest to other land cover types).

The changes in area and spatial distribution of various forest types within Changting County, conservation zones, and non-conservation zones are presented in Table 4 and Figure 5. The results show that, from 2010 to 2021, unchanged forestlands accounted for the largest portion (about 40% of the land) in all three statistical zones, while Masson pine expansion (i.e., converted from other land cover types) accounted for the second largest portion. Particularly, the percentage of increased Masson pine in the conservation zones was much greater (29.2%) than that in the non-conservation zones (17.8%). The opposite situation occurred with Chinese fir and broadleaf forests, whose increased areas were relatively lower in the conservation zones than in the non-conservation zones. This also confirmed that Masson pine played an important role in ecological restoration in the soil erosion area [57].

**Table 4.** Change areas (ha) and proportions (%) of various forest types between 2010 and 2021.

Forest Change Category	Statistical Units		
	Changting County Area (ha) (%)	Conservation Zones Area (ha) (%)	Non-Conservation Zones Area (ha) (%)
Increased Masson pine	58,603 (18.9)	9444 (29.2)	49,614 (17.8)
Increased Chinese fir	22,919 (7.4)	924 (2.9)	21,788 (7.8)
Increased broadleaf forest	46,273 (14.9)	1928 (6.0)	43,882 (15.8)
Increased bamboo forest	6584 (2.1)	743 (2.3)	5843 (2.1)
Forest loss	9037 (2.9)	1279 (4.0)	7875 (2.8)
Unchanged forests	126,398 (40.7)	12,913 (40.0)	113,698 (40.9)
Other changes	40,745 (13.1)	5068 (15.7)	35,562 (12.8)
Total	310,560 (100.0)	32,298 (100.0)	278,261 (100.0)

#### 4.2. FVC Change Trends over Time

The annual FVC results from 1986 to 2021 (Figure 6a) showed that the average FVC values in the non-conservation zones were higher than in the conservation zones; both exhibited increasing trends, but the increase rate is different, especially after 2010. In 1986, the average FVC in the conservation zones was only 38%, but it reached 72% in 2021 after decades of implementing soil and water conservation practices. Before 2010, the annual average FVC in the conservation zones grew slowly, and the yearly growth rate was only 0.76%, but it reached 1.81% after 2010. In contrast, the average FVC in the non-conservation zones was 67% in 1986 and reached 80% in 2021, with an annual growth rate of only 0.36%. The discrepancy regarding average FVC between the conservation and non-conservation zones has shrunk significantly from 31% in 1986 to 10% only in 2021, and the FVC values became gradually closer to each other. We also found that the lowest FVC values during 1988–1994 corresponded to some historical events. During this period, the first wave of rare mineral mining began, causing a large scale of vegetation damage in Hetian Township and its surrounding areas; the whole region launched comprehensive development of mountainous areas, planting fruit trees on hills without keeping up with the necessary protective measures, resulting in soil erosion [58].

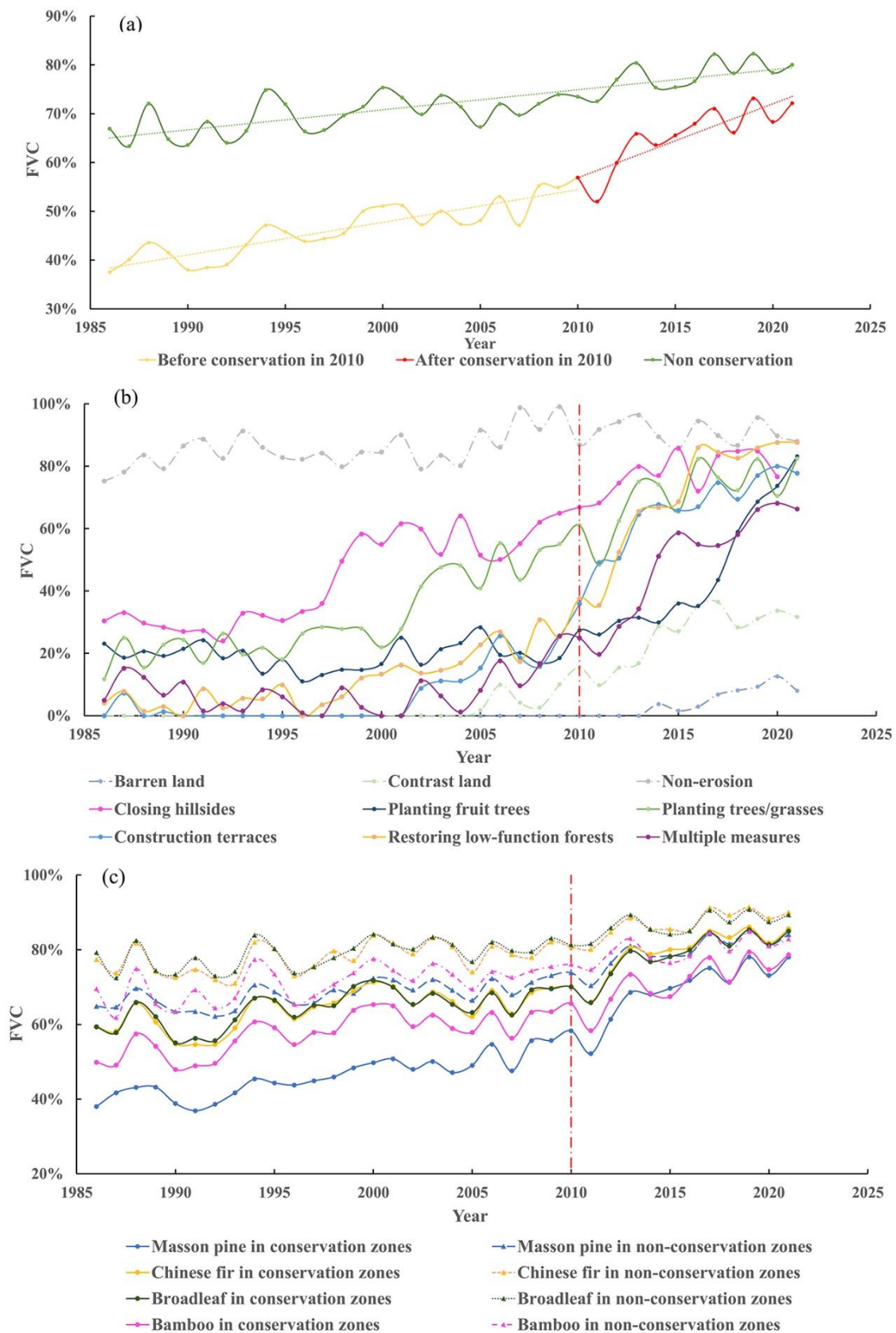


**Figure 6.** The fractional vegetation cover (FVC) change trends from 1986 to 2021 in conservation zones and non-conservation zones ((a)—average annual FVC; (b)—FVC trends in different conservation measures and different situations without conservation; (c)—a comparison of FVC curves of different forest types between conservation and non-conservation zones).

Analysis of the FVC curves from 1986 to 2021 (Figure 6b) based on representative sites with different conservation measures in the conservation zones and non-conservation zones indicated that the FVC changes over time had significantly different patterns. In the non-conservation zones, the FVC generated various patterns due to the initial vegetation conditions. For 'non-soil erosion' with high vegetation cover, the FVC was relatively stable at about 80% averagely, presenting a flat pattern; for 'contrast land', the FVC was continuously low at the beginning, but it gradually increased and reached about 40% after 2005, belonging to a vee pattern. The worst situation went to 'barren land' with no vegetation cover, whose FVC stayed as low as 0% for a long time; it increased after 2014 but still stayed less than 10%, manifesting a flat pattern in general. The FVC increases in 'barren land' and 'contrast land' after 2014 may be attributed to the overall improvement in local ecological quality and microclimate changes after conservation measures were implemented. Previous research [59] showed that restored vegetation, especially forests in the soil-eroded areas, has significant effects on near-surface temperature, humidity, daily temperature variation, soil temperature, and soil moisture, creating better local microclimates and a significantly improved ecological environment in the region. It is worth noting that the low FVC values of 'barren land' and 'contrast land' imply that vegetation restoration relying on only natural processing to reach a desirable level in those areas takes a very long time without proper human efforts.

The FVC curves in the conservation zones were greatly different from those of the non-conservation zones. In general, FVC largely increased during 1986–2021 but presented various change paces among different conservation measures, reflected by various inflection points of FVC change because of the dates when conservation measures were implemented, in particular, around 2010. Figure 6b showed that, during the early years of the study period, the FVC remained stable and, after some time, the FVC increased steadily or sharply at different rates under conservation measures, presenting increasing or vee patterns. For example, in the 'closing hillsides' implemented site, the initial FVC was relatively high and stable at about 30% until 1997, and it sharply increased to about 60% in 1999, then kept on for a couple of years with some fluctuations; after 2010, the FVC gradually grew and stabilized at about 80%. For the site with 'planting trees and grass', the FVC remained stable until 2000, then gradually increased, while, with 'planting fruits', the FVC sharply increased after 2015. For the sites with 'restoring low-function forest', 'constructing terraces on slope lands', and 'multiple control measures', the FVC experienced dramatic increases after 2010, especially for 'restoring low-function forest'. The FVC reached its highest at about 80% in 2021, similar to the case of 'non-soil erosion', indicating the high effectiveness of the 'restoring low-function forest' conservation method. The FVC under 'multiple control measures' was lower than the FVC values of other conservation measures, implying the obstinateness of those areas to be controlled effectively.

These FVC change patterns were very closely related to the characteristics of the conservation measures and the particular dates. The 'closing hillsides' measure was the earliest and most practiced in Changting County because it is the most economical, effective, and quickest approach, especially to control light and moderate soil erosion and to consolidate the management result. According to the report [58], during 1999–2009, 'closing hillsides' was carried out on an area of 65,000 ha, accounting for 84% of the total conservation area of 77,400 ha during the same period. Therefore, the FVC increase inflection occurred the earliest among the various measures. The tenure reform of collective forests in 1994 warranted villagers 50-year rights to freely use their allocated hilly lands, starting the 'first planting grass, then trees' conservation mode; consequently, the FVC increased slowly at the beginning (around 1995–2000), then sharply raised following the tree growth patterns. A large scale of 'restoring low-function forest', which promotes tree growth by fertilizing and tending, was implemented after 2010, and, corresponding to this date, the FVC quickly rose after 2010. The practice of planting fruits (including other cash shrubs, e.g., camellia) in a large area also started in 2012; due to the large space between

fruit trees, the FVC in the first couple of years did not change obviously, then increased quickly after 2015.

The yearly average FVC change for various forest types at typical sites selected from the land cover map of 2021 in both the conservation zones and the non-conservation zones from 1986 to 2021 (Figure 6c) clearly shows that, among the forest types, broadleaf and Chinese fir forest have similar FVC values, which are higher than Masson pine and bamboo forests in both the conservation zones and non-conservation zones. This can be attributed to the fertile soil conditions in which broadleaf and Chinese fir forests typically grow and the characteristics of the tree species. The FVC values of all the forest types in the non-conservation zones were higher than those in the conservation zones. Even in the early stages of conservation efforts, the differences in FVC values were significant, ranging from 20% to 30%. However, after 2010, the differences in FVC values between the same forest types gradually reduced to 5–8% in 2021. The FVC of all forest types in the non-conservation zones fluctuated, with slight growing trends over the entire study period. In contrast, the FVC values in the conservation zones fluctuated but were unchanged or slowly increased before 2010 and dramatically increased after 2010 when conservation measures were implemented. Although FVC increased rapidly for all the forest types in the conservation zones, the rates of increase varied significantly among different forest types. The FVC in 2021 increased by 33.9% for Masson pine, 22.2% for Chinese fir, 21.3% for broadleaf, and 20.0% for bamboo compared to 2010. In contrast, the corresponding increases in FVC for the same forest types in the non-conservation zones were 13.8%, 11.4%, 9.9%, and 8.9%, respectively. At the end of the study period, the FVC differences between different forest types became narrower. For example, the FVC values of Masson pine and bamboo forests were similar but still lower than those of broadleaf and Chinese fir forests in the conservation zones. However, the FVC values of broadleaf and Chinese fir forests reached as high as those of Masson pine and bamboo forests in the non-conservation zones. The considerable FVC differences between the conservation and non-conservation zones prior to the governance and the reduced gap after imply the important role of implementing conservation measures for improving FVC, thus reducing soil erosion problems.

#### *4.3. Effects of the Conservation Measures on Land Cover Changes*

The areas and proportions of different land cover types under different conservation measures in the conservation zones and non-conservation zones in 2021 (Table 5) showed that Masson pine forests accounted for the largest portion (64–84%) of the total area under the corresponding conservation measures, while other forests accounted for a smaller portion (<10%), especially for cases with ‘multiple control measures.’ Over the past decade, conservation efforts have led to the establishment of Masson pine-dominated forests in most soil erosion areas in the conservation zones. In comparison, Masson pine forests accounted for a relatively small portion (about 45%) in the non-conservation zones, while Chinese fir and broadleaf forests made up 9.4% and 28.0%, respectively. Through conservation efforts, bare land areas in the conservation zones are much smaller than in the non-conservation zones, especially in the categories of ‘restoring low-function forest’ and ‘multiple control measure.’ However, there were still some bare lands uncovered in the area of ‘closing hillsides to facilitate afforestation.’ It is important to note that ‘closing hillsides’ relies on the natural regeneration ability of vegetation to restore its original condition gradually. This is achieved by prohibiting any forms of intrusion, such as reclamation, grazing, and firewood cutting. In areas with severe soil erosion, the harsh soil and water conditions make it difficult for plants to survive and grow. Therefore, it is impossible to turn barren land into forests solely through the natural regeneration ability in a short time period. In some cases, human investment is necessary to obtain satisfactory results. The small area of bare land under ‘multiple control measures’ demonstrates that proper investment of labor and resources in water and soil erosion control can enhance conservation outcomes.

**Table 5.** Areas (ha) and proportions (%) of land cover types and their changes under different conservation measures.

Land Cover Types		Different Conservation Measures				
		Restoring Low-Function Forest	Closing Hillside	Planting Trees and Grass	Multiple Measures	Non-Conservation
Classification results for 2021	Masson pine	957 (71.1)	15,730 (63.7)	3451 (74.6)	1229 (84.4)	124,416 (44.7)
	Chinese fir	29 (2.2)	845 (3.4)	73 (1.6)	12 (0.8)	26,158 (9.4)
	Broadleaf forest	100 (7.4)	2365 (9.6)	285 (6.2)	42 (2.9)	77,811 (28.0)
	Bamboo forest	44 (3.3)	574 (2.3)	122 (2.6)	19 (1.3)	6461 (2.3)
	Farmland	31 (2.3)	641 (2.6)	98 (2.1)	15 (1.0)	9099 (3.3)
	Bare land	81 (6.0)	1959 (7.9)	316 (6.8)	72 (4.9)	14,274 (5.1)
	Water	10 (0.7)	166 (0.7)	15 (0.3)	8 (0.5)	2352 (0.8)
	Impervious surface area	94 (7.0)	2431 (9.8)	263 (5.7)	61 (4.2)	17,691 (6.4)
	Total	1347 (100.0)	24,711 (100.0)	4625 (100.0)	1457 (100.0)	278,262 (100.0)
	Change detection results between 2010 and 2021	Increased	323 (24.0)	7066 (28.6)	1476 (31.9)	542 (37.2)
Increased		29 (2.2)	813 (3.3)	72 (1.6)	12 (0.8)	21,788 (7.8)
Increased		88 (6.5)	1564 (6.3)	235 (5.1)	35 (2.4)	43,882 (15.8)
Increased		43 (3.2)	551 (2.2)	119 (2.6)	19 (1.3)	5843 (2.1)
Forest loss		45 (3.3)	1021 (4.1)	164 (3.6)	39 (2.7)	7875 (2.8)
Unchanged forest		648 (48.1)	9532 (38.6)	2033 (44.0)	696 (47.7)	113,698 (40.9)
Other changes		170 (12.6)	4164 (16.9)	526 (11.4)	115 (7.9)	35,562 (12.8)
Total		1347 (100.0)	24,711 (100.0)	4625 (100.0)	1457 (100.0)	278,262 (100.0)

In terms of changes in land cover within conservation zones, all the conservation measures generally protected the existing forests and expanded the Masson pine forests. According to Table 5, the proportions of unchanged forests under different conservation measures ranged from 38.6% to 48.1%. Only small proportions of forests were lost or degraded to other land cover types, such as farmland, ISA, or bare land. Among the different conservation measures, ‘closing hillsides’ resulted in the largest expansion of Masson pine forests (by 7065 ha). Following Masson pine, broadleaf forests were the second largest forest type that expanded under various conservation measures.

#### 4.4. Effects of the Conservation Measures on FVC Changes

##### 4.4.1. Comparison of FVC Change Patterns and Magnitudes at Spatial Scales

The areas and proportions of the FVC change patterns and magnitudes within Changting County, the conservation zones, and the non-conservation zones (Table 6) and their spatial distributions (Figure 7) indicated that, in terms of change patterns, FVC presented growth trends generally in the entire county, revealed by the highest percentages of increasing shape (49.0%) and vee shape (12.1%). About 17.7% of Changting County did not change much in FVC (the flat shape), while only small areas (6.7%) experienced FVC reduction (2.6% decreasing pattern and 4.1% inverse vee pattern), and 14.5% of the area underwent large fluctuations (the jump shape) during the study period. The FVC-reducing areas were mainly located around towns with more human activities and were distributed in strips, while the jump patterns were widely distributed, mainly in the west of Changting, where the ecological environment is better. In addition, the flat pattern and the decreasing pattern were often accompanied by each other in space. The comparison of change patterns between the conservation and non-conservation zones indicated that the total proportion of growing patterns (increasing and vee shapes) made up 70.7% of the conservation zones, which is higher than 60.0% in the non-conservation zones. This demonstrated the great effect of the conservation measures on vegetation recovery.

**Table 6.** The area (ha) and percentage (%) of fractional vegetation cover (FVC) change patterns and intensities in Changting County, conservation zones, and non-conservations zones.

FVC Change Patterns		Changting County	Conservation Zones	Non-Conservation Zones
Change patterns	Flat	54,969 (17.7)	1442 (4.5)	53,527 (19.2)
	Decreasing	7950 (2.6)	298 (0.9)	7652 (2.7)
	Increasing	152,205 (49.0)	12,772 (39.5)	139,433 (50.1)
	Vee	37,702 (12.1)	10,068 (31.2)	27,634 (9.9)
	Inverse vee	12,764 (4.1)	5024 (15.6)	7740 (2.8)
	Jump	44,969 (14.5)	2694 (8.3)	42,275 (15.2)
Change intensities	Non-change	59,721 (19.2)	1920 (5.9)	57,801 (20.8)
	Light	39,958 (12.9)	1098 (3.4)	38,860 (14.0)
	Moderate	81,578 (26.3)	4627 (14.3)	76,951 (27.7)
	Severe	68,139 (21.9)	8275 (25.6)	59,864 (21.5)
	Extreme	61,164 (19.7)	16,378 (50.7)	44,786 (16.1)
Total		310,560 (100.0)	32,298 (100.0)	278,262 (100.0)

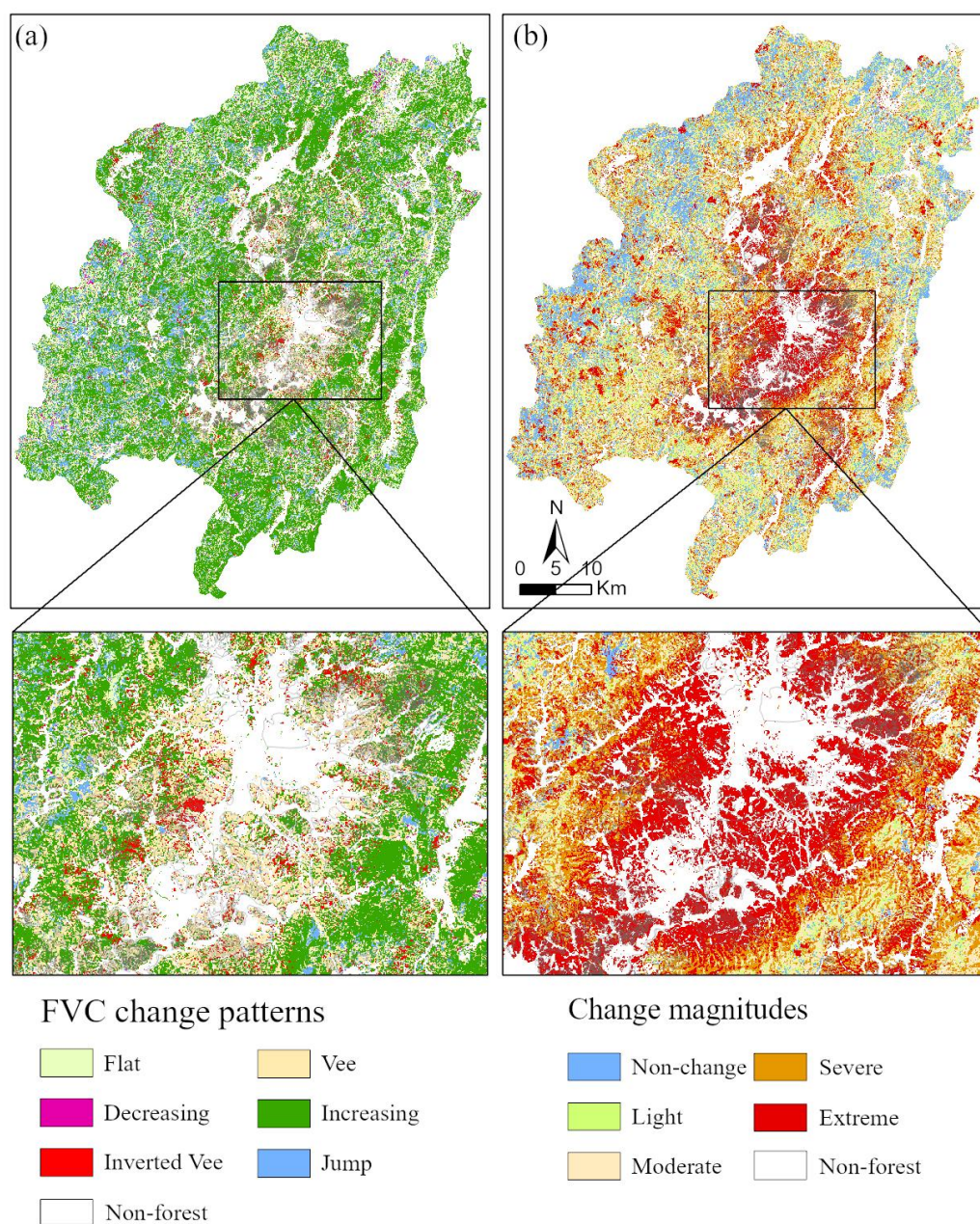


**Figure 7.** The change patterns and change magnitudes in fractional vegetation cover (FVC) from 1986 to 2021 in Changting County, Fujian Province ((a)—change patterns; (b)—change magnitudes).

Regarding the change magnitudes, one third of the entire county did not experience strong disturbances and the FVC did not change obviously (no change and light), while the rest of the land underwent strong degrees of FVC changes at some time points between 1986 and 2021, of which the moderate degree accounted for the largest portion, followed by severe and extreme. The FVC change intensities in the conservation zones and non-conservation zones appeared to be very different. For example, the change magnitude at severe and extreme levels accounted for 76.3% of the conservation zones and only 37.6% of the non-conservation zones. In contrast, no change and light accounted for 9.3% of the conservation zones and 34.8% of the non-conservation zones. This also confirmed that the conservation action significantly stimulated vegetation coverage changes.

Comprehensive analysis of change patterns and magnitudes indicated that flat change patterns were associated with non-change intensity, increasing patterns were associated with light and moderate change intensities, and vee, inverse vee, and jump patterns were

associated with severe and extreme change intensities. These high agreements may be attributed to the definitions of the change patterns and change intensities based on FVC value changes.

#### 4.4.2. Effects of Different Conservation Measures on FVC Change Patterns and Magnitudes

Within the conservation zones, the compositions of FVC change patterns varied under different conservation measures (Table 7). For example, under the ‘restoring low-function forest’ and ‘closing hillsides’ measures, the FVC change patterns are similar, with the increasing shape being the largest, followed by vee, inverse vee, jump, flat, and decreasing patterns. However, for ‘planting trees and grass’ and ‘planting fruit trees’, the order of increasing shape and vee shape was reversed. The ‘constructing terraces’ conservation measure had a different pattern of FVC change compared to the four other measures mentioned above. The vee shape accounted for a large proportion of 63.0%, followed by the inverse vee (17.2%) and increasing shape (14.7%), while the other patterns accounted for a relatively small portion. With the ‘multiple measures’ conservation approach, the growing patterns accounted for the largest portion of 77.7%, of which the vee shape accounted for 48.4%, and the decreasing and flat patterns accounted for the smallest portion.

**Table 7.** Areas (ha) and proportions (%) of fractional vegetation cover (FVC) change patterns under different conservation methods.

Conservation Measures	Patterns of FVC Change						Total
	Flat	Decreasing	Increasing	Vee	Inverse Vee	Jump	
Restoring low-function forests	75 (5.6)	12 (0.9)	586 (43.5)	378 (28.1)	216 (16.0)	80 (5.9)	1347 (100.0)
Closing hillsides	1196 (4.8)	262 (1.1)	10,164 (41.1)	7006 (28.4)	3778 (15.3)	2306 (9.3)	24,711 (100)
Planting trees and grass	153 (3.3)	19 (0.4)	1591 (34.4)	1885 (40.8)	730 (15.8)	247 (5.3)	4625 (100.0)
Planting fruit trees	2 (6.9)	0.4 (1.5)	7 (25.6)	11 (42.7)	4 (14.5)	2 (8.6)	26 (100.0)
Constructing terraces	4 (2.8)	0.4 (0.3)	19 (14.7)	83 (63.0)	23 (17.2)	3 (2.0)	131 (100.0)
Multiple measures	12 (0.8)	5 (0.3)	405 (27.8)	705 (48.4)	273 (18.8)	56 (3.9)	1457 (100.0)
Total conservation zones	1442 (4.5)	298 (0.9)	12,772 (39.5)	10,068 (31.2)	5024 (15.6)	2694 (8.3)	32,298 (100.0)
Non-conservation	53,527 (19.2)	7652 (2.7)	139,433 (50.1)	27,634 (9.9)	7740 (2.8)	42,275 (15.2)	278,262 (100.0)

The common characteristics of the conservation measures ‘planting trees and grass’, ‘planting fruit trees’, ‘constructing terraces’, and ‘multiple control measures’ are that the vee shape accounted for the largest portion (40.8–63.0%), which was significantly higher than that in non-conservation zones. The vee shape represents a situation where FVC remained unchanged or decreased for a long time and then increased. In the conservation zones, the areas affected by soil erosion often have little to no vegetation cover, resulting in a stable FVC value at the beginning of the study period. After implementing conservation measures, FVC gradually increased, exhibiting the vee pattern, indicating the effectiveness of these measures regarding vegetation recovery. The inverse vee shape is associated with a situation where FVC increased for a period and then experienced a downward trend. In the conservation zones, this pattern reflects the recurrence of soil erosion in some areas, which is confirmed by the large proportion of the inverse vee pattern under the ‘multiple measures’ approach.

All the conservation measures inevitably caused FVC change intensively. The percentages of change magnitude levels under each conservation measure (Table 8) showed

that extreme change in FVC accounted for the largest portion (38.6–84.0%) under all the conservation measures, except for ‘restoring low-function forest’ and ‘closing hillsides’; extreme change made up over 60% under the other conservation methods. Severe changes were the second largest allocations among the magnitude levels, while no change, light, and moderate levels accounted for small portions. According to Table 8, ‘restoring low-function forest’ and ‘closing hillsides’ had a similar effect on the FVC change intensities, while the four other conservation measures were similar.

**Table 8.** Areas (ha) and proportions (%) of fractional vegetation cover (FVC) change magnitudes under different conservation methods.

Conservation Measures		Magnitudes of FVC Changes					Total
		No Change	Light	Moderate	Severe	Extreme	
Conservation measures	Restoring low-function forests	111 (8.2)	27 (2.0)	216 (16.0)	473 (35.1)	520 (38.6)	1347 (100.0)
	Closing hillsides	1579 (6.4)	1013 (4.1)	3932 (15.9)	6480 (26.2)	11,708 (47.4)	24,712 (100.0)
	Planting trees and grass	204 (4.4)	53 (1.1)	405 (8.8)	1034 (22.4)	2929 (63.3)	4625 (100.0)
	Planting fruit trees	5 (19.2)	0 (0)	1 (3.8)	2 (7.7)	18 (69.2)	26 (100.0)
	Constructing terraces	5 (3.8)	0 (0)	4 (3.1)	13 (9.9)	110 (84.0)	131 (100.0)
	Multiple measures	16 (1.1)	4 (0.3)	71 (4.9)	273 (18.7)	1093 (75.0)	1457 (100.0)
	Total conservation zones	1920 (5.9)	1098 (3.4)	4627 (14.3)	8275 (25.6)	16,378 (50.7)	32,298 (100.0)
Non-conservation zones	57,801 (20.8)	38,860 (14.0)	76,951 (27.7)	59,864 (21.5)	44,786 (16.1)	278,262 (100.0)	

Analysis of the boxplot of the FVC change magnitude with different conservation measures (Figure 8) revealed that both the mean and median FVC change magnitudes in the conservation zones were much higher than those in the non-conservation zones. This suggests a clear effect of conservation on vegetation restoration. When comparing the various conservation measures, it was found that ‘restoring low-function forest’ and ‘closing hillsides’ had similar FVC change magnitudes, with mean values of about 0.50. This was lower than the FVC change magnitudes of ‘planting trees and grass’ and ‘planting fruit trees’ at 0.6 and ‘constructing terraces’ and ‘multiple measures’ at 0.67. Among the conservation measures, ‘multiple measures’ specifically targeting recurrent and severe soil erosion areas resulted in the highest FVC change magnitude. This indicates that the input of labor and resources in these areas achieved the greatest success in vegetation restoration.

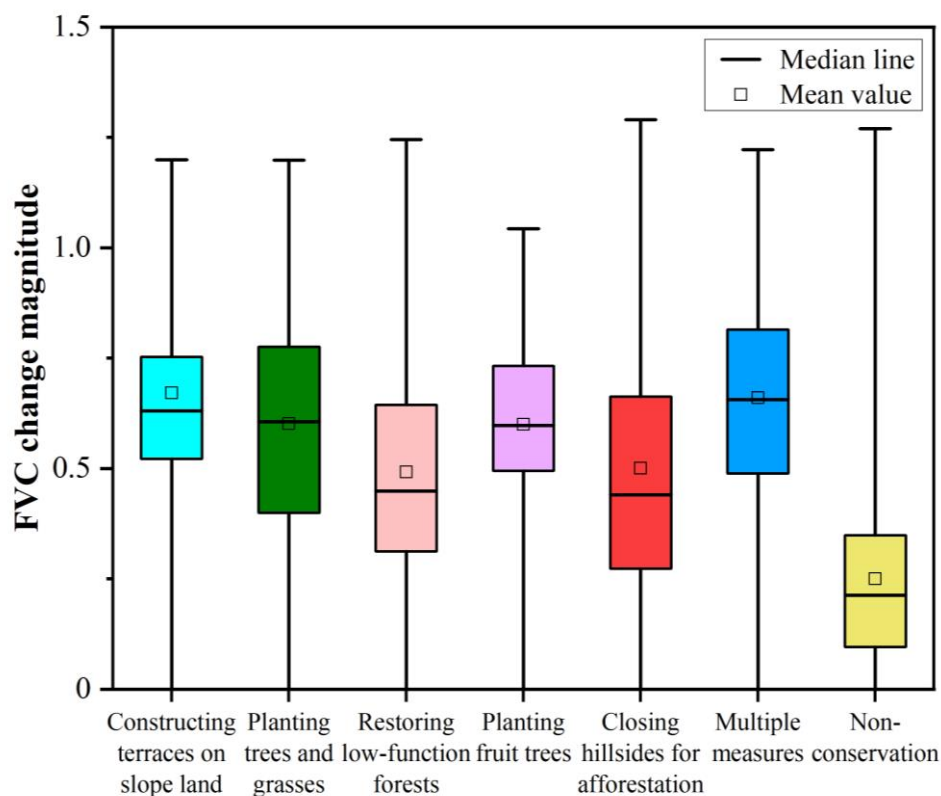


**Figure 8.** Boxplot of fractional vegetation cover change magnitudes under different conservation measures.

#### 4.5. Effects of Different Conservation Measures on FVC Change Patterns and Magnitudes of Major Forest Types

##### 4.5.1. FVC Change Patterns of Major Forest Types under Different Conservation Measures

The areas and areal percentages of FVC change patterns of different forest types under different conservation measures were computed and presented in Table 9. Because of the small areas of bamboo forests, and the implemented ‘planting fruit trees’ and ‘constructing terraces’, they were not included in the analysis. In different conservation measures, the FVC change patterns for the forest types were dominated by the vee and increasing shapes, accounting for the largest portions (78.8–89.4%), which were much higher than those of the same forest types in the non-conservation zones (61.9–69.6%). However, there were some differences among the conservation measures. Under the ‘restoring low-function forest’ and ‘closing hillsides’ measures, the proportions of increasing shape were higher than the vee shape for all the forest types. Moreover, ‘restoring low-function forest’ was carried out on the moderate and severe soil erosion areas by fertilizing and tending to improve the growth of Masson pine, Chinese fir, *Schima superba*, and *Liquidambar styraciflua*, while ‘closing hillsides’ involved the enforced closure of the designated areas to promote the natural growth of forests and vegetation recovery, mainly Masson pine. With ‘planting trees and grass’ and ‘multiple measures’, the vee shape accounted for larger portions than the increasing shape for Masson pine forests because Masson pine is tolerant to poor soil and is one of the tree species to plant for soil erosion control. In terms of forest types, the largest proportion of inverse vee shape was associated with Masson pine, accounting for 8–10% under all the conservation measures, which was larger than for Chinese fir and broadleaf forests. The flat shape and jump shape were more related to broadleaf forests under most of the conservation measures.

**Table 9.** Areas (ha) and proportions (%) of FVC change patterns of forest types under different conservation methods.

Conservation Methods	Forest Types	Patterns of FVC Change						Total
		Flat	Decreasing	Increasing	Vee	Inverse Vee	Jump	
Restoring low-function forests	Masson pine	48 (5.0)	4 (0.4)	471 (49.2)	313 (32.7)	77 (8.0)	46 (4.8)	958 (100.0)
	Chinese fir	1 (2.0)	0 (0.0)	17 (57.5)	9 (31.9)	1 (4.7)	1 (4.0)	29 (100.0)
	Broadleaf forest	7 (7.2)	0.2 (0.2)	61 (60.7)	23 (22.7)	4 (4.0)	5 (5.1)	100 (100.0)
Closing hillsides	Masson pine	661 (4.2)	71 (0.5)	7264 (46.1)	5456 (34.7)	1225 (7.8)	1069 (6.8)	15,746 (100.0)
	Chinese fir	37 (4.4)	2 (0.2)	523 (61.8)	194 (22.9)	25 (2.9)	66 (7.8)	848 (100.0)
	Broadleaf forest	160 (6.8)	15 (0.6)	1390 (58.8)	497 (21.0)	75 (3.2)	228 (9.7)	2365 (100.0)
Planting trees and grass	Masson pine	77 (2.2)	6 (0.2)	1316 (38.1)	1610 (46.6)	299 (8.7)	146 (4.2)	3454 (100.0)
	Chinese fir	3 (4.2)	0.1 (0.1)	39 (52.9)	23 (31.5)	3 (4.1)	5 (7.2)	74 (100.0)
	Broadleaf forest	20 (7.0)	0.3 (0.1)	161 (56.5)	72 (25.3)	13 (4.6)	18 (6.5)	285 (100.0)
Multiple measures	Masson pine	5 (0.4)	2 (0.1)	412 (33.5)	646 (52.5)	125 (10.2)	41 (3.3)	1230 (100.0)
	Chinese fir	0 (0)	0 (0)	5 (44.4)	5 (41.3)	1 (8.0)	1 (6.3)	12 (100.0)
	Broadleaf forest	0.4 (1.0)	0.1 (0.1)	22 (52.3)	15 (36.5)	3 (7.9)	1 (2.1)	42 (100.0)
Non-conservation	Masson pine	20,541 (16.5)	2177 (1.7)	65,281 (52.5)	16,722 (13.4)	3621 (2.9)	16,087 (12.9)	124,428 (100.0)
	Chinese fir	4243 (16.2)	228 (0.9)	15,187 (58.1)	2998 (11.5)	233 (0.9)	3270 (12.5)	26,158 (100.0)
	Broadleaf forest	15,516 (19.9)	1253 (1.6)	41,069 (52.8)	7073 (9.1)	942 (1.2)	11,960 (15.4)	77,811 (100.0)

#### 4.5.2. FVC Change Magnitudes of Major Forest Types under Different Conservation Measures

The variations in the FVC change magnitudes of the major forest types under different conservation measures (Figure 9) indicated that the FVC change magnitudes (median and mean) of all the forest types in the conservation zones were larger than those in the non-conservation zones. When the same conservation measure was implemented, the FVC of Masson pine forests changed the most dramatically compared with those of Chinese fir and broadleaf forests, while Chinese fir forests and broadleaf forests were similar. For example, under ‘closing hillsides’ conservation, the median FVC change magnitude of Masson pine forests was 0.48, while it was 0.33 for Chinese fir and 0.31 for broadleaf forest. However, different conservation measures had greatly different impacts on the magnitude of FVC change. Indeed, ‘multiple measures’ resulted in the highest FVC change magnitude for all three forest types (median values 0.48–0.68), followed by ‘planting trees and grass’ (median 0.40–0.61), while ‘restoring low-function forest’ (median 0.22–0.30) and ‘closing hillsides’ (median 0.19–0.29) had relatively lesser effects on the FVC change magnitudes. Among all the forest types and conservation methods, the FVC of Masson pine forests under ‘multiple measures’ changed the most, suggesting that Masson pine forests under ‘multiple measures’ had the greatest effect on vegetation restoration.

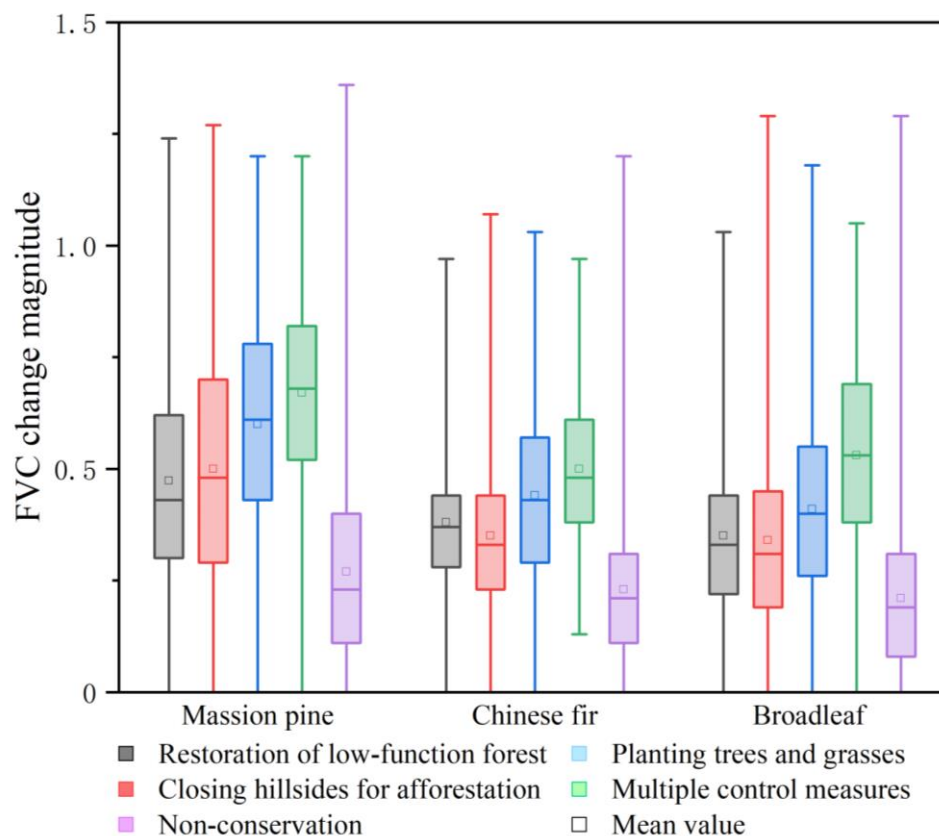


**Figure 9.** The change magnitudes of fractional vegetation cover (FVC) of major forest types under different conservation measures.

## 5. Discussion

### 5.1. Importance of Improving Vegetation Structure and Composition in Reducing Soil Erosion Problems

Vegetation restoration is a promising strategy to control soil erosion and improve ecosystem services from small watersheds to large regions [60]. Increasing vegetation cover can considerably reduce soil erosion, while decreasing vegetation cover may cause increased runoff and soil loss [61]. In general, when the vegetation cover rate is greater than 70%, soil erosion will be effectively controlled. This study evaluated the impact of various conservation measures on FVC changes in soil erosion areas. Compared with previous studies assessing the effectiveness of soil and water conservation [62] and the spatial variations in soil and water loss, this study emphasized the FVC dynamic changes of different forest types under various conservation measures, thus better revealing the responses of FVC change to different conservation measures during vegetation recovery and soil erosion control. The spatial and temporal changes in FVC based on a long-term Landsat time series in Changting County are consistent with previous research [63]. After conservation was implemented, the FVC in intensively eroded areas increased sharply, with a rate of 90%, much better than in non-conservation areas, implying an immediate effect of the management practices in terms of reducing soil erosion problems.

Based on time series FVC data, the “ShapeSelection” algorithm [55] was used to examine the FVC change pattern and intensity at the pixel level, providing detailed spatial and temporal information regarding vegetation changes and intuitively showing where soil erosion situations were mitigated or controlled with a particular conservation measure and where they still needed intensive management. For example, vee patterns of FVC change, which are mainly distributed in the Hetian Basin and represent sharp increases in vegetation coverage, indicate that these areas achieved the best outcomes regarding the conservation efforts, while the inverse vee patterns of FVC changes were found in the

hinterland of the Hetian Basin, where the soil erosion problems recur year after year and thus require intensive control practices with multiple control measures.

Except for vegetation cover, vegetation types, vegetation diversity, and vegetation structure, the vertical forest structure also particularly influences runoff and soil erosion [64]. In Changting County, the large area of regenerated or planted Masson pine forests and high-value fruit trees significantly increased the vegetation coverage and achieved remarkable success in controlling soil erosion problems [65]. However, because of the lack of understory vegetation or litter to closely cover the surface soil, soil erosion still occurred moderately or even severely in some forested areas [66]. Therefore, to better control under-forest soil erosion, it requires not only increasing the vegetation cover but also optimizing the forest compositions and structures [67]. Mixed forests or multi-layered vegetation compositions with complex vertical forest structures can largely increase rainfall interception, mitigate the raindrop impact on the ground, and reduce runoff. They are more efficient than monoculture in restoring eroded land and enhancing soil fertility [68]. Currently, Masson pine forests account for the largest portion of all the forests in Changting County. The spread of destructive pine wilt disease among the Masson pine forests and high fire risk are serious threats to the great achievement of decades of soil erosion control. Thus, transformation of pure and low-quality Masson pine forests into mixed pine and broadleaf forests or into forests with high structural diversity may be an optimal conservation method in the future, not only increasing vegetation cover and structure but promoting biodiversity of forest ecosystems.

### *5.2. Effects of Different Conservation Measures on Improving Forest Coverage*

Increasing vegetation cover is essential for soil erosion control. However, different conservation measures have various effects on vegetation cover recovery. This study found that three conservation methods, i.e., ‘multiple control measures’, ‘constructing terraces’, and ‘planting trees and grass’, enabled trees or grass to grow in the regions with dominant bare soils where natural vegetation restoration was difficult. The FVC increased from a very low level to about 70% in a relatively short time period, and this region turned the previous “flame mountains” into green forests; a similar result was achieved in previous research conducted by Zhang et al. [69]. Among the various control measures, ‘multiple control measures’ brought the largest changes in FVC, which is also consistent with the previous research finding that the combined use of multiple control measures in areas with severe soil erosion is effective [70]. ‘Planting trees and grass’ and ‘planting fruit trees’ led to a moderate intensity of FVC changes, while ‘closing hillsides’ and ‘restoring low-function forests’ resulted in the least intensity of FVC changes due to less involvement regarding human activities. Those measures were more suitable to the light and moderate soil erosion conditions.

Different conservation measures affected the FVC change patterns and magnitudes. The percentage of the inverted vee shape in the FVC change pattern under ‘multiple control measures’ was the highest among all the conservation measures. Although ‘multiple control measures’ proved to be very effective in increasing vegetation cover, major labor input, material, money, and time were required. Therefore, caution should be taken regarding the areas where soil erosion recurred after one and another type of control method were implemented. The ‘closing hillsides’ measure is the least effective among all the conservation measures in terms of vegetation cover recovery because it relies on the capability of natural regeneration by restricted or prohibited human intervention to promote vegetation establishment from natural seed fall, achieving the goal of soil erosion control. It does not require much human input but takes longer to allow vegetation to recover to the level at which soil erosion can be effectively controlled. Therefore, it is more suitable on a large scale, especially in areas where environmental conditions such as temperature and rainfall are favorable. This research implies that the measures taken to control soil erosion should consider the soil and original vegetation conditions, and cost and labor needed, in addition to soil erosion severity.

### 5.3. Limitations of the Research and Perspective for Future Work

The analyses of FVC change trends and change patterns in this research relied solely on FVC derived from the Landsat time series. Cloud cover on the Landsat image is a major issue in the subtropical region due to the frequent rainy and cloudy weather, which limits the number of valid pixels to form accurate yearly NDVI time series. The lack of usable Landsat 7 ETM+ images led to missing data for 2012, which were filled with the averages of 2011 and 2013. The calculation of FVC from NDVI involves the determination of  $NDVI_{veg}$  and  $NDVI_{soil}$  values (Equation (1)), which was likely an arbitrary decision, although the choice was based on statistical metrics. Thus, the FVC time series itself already has some uncertainty.

The ShapeSelectionForest algorithm used in this study to identify FVC change patterns based on FVC time series did not consider meteorological effects such as rainfall and extreme temperature, which greatly impact vegetation growth, inducing unreasonable fluctuation in NDVI along time. Thus, the resulting FVC change patterns or magnitudes may contain some discrepancies. Due to a lack of ground truth data, those patterns cannot be validated properly. Therefore, the methodology used in this research has the potential to be improved regarding both the data source and algorithm. Incorporating different sensors is a promising way to enhance the data availability.

Soil and water management is a long-term and arduous task and requires a comprehensive analysis of the local environmental conditions and economic and cultural activities, based on which a scientific management plan is formulated. According to soil erosion situations, the key prevention areas that are highly prone to soil erosion and the key control areas where serious soil erosion occurs are mapped out, and suitable conservation measures targeting different situations are created and implemented. It is also important to monitor the governance effect, ensuring quality of management. In Changting County, after 30 years of conservation efforts, soil erosion has been considerably controlled. However, some re-greened areas still have a probability of suffering secondary soil erosion. Thus, it is necessary to continuously monitor vegetation growth, such as FVC change.

## 6. Conclusions

This study analyzed the land cover changes and FVC dynamics using time series Landsat imagery after different soil and water conservation measures were implemented in Changting County, Fujian Province. The results show a considerable increase in Masson pine forest with a significant decrease in bare soils. The overall FVC increases all over the county, especially average FVC, are higher in the non-conservation regions than in the conservation regions, but the increase rate is inverse, especially since 2010 with the implementation of soil and water conservation measures, implying the important role of conservation measures in reducing soil erosion problems and restoration of forest coverage. The FVC change magnitudes show ‘planting trees and grass’ and ‘constructing terraces’ have better performance in improving FVC than ‘restoring low-function forest’ and ‘closing hillsides’. Of the different conservation measures, ‘multiple measures’ has the highest change magnitudes, implying the largest impact of this measure on FVC change, but the higher “inverse vee” patterns than other measures indicate difficulty regarding improving forest coverage, thus requiring more attention for these regions.

**Author Contributions:** Conceptualization, D.L. (Dengsheng Lu) and Q.W.; methodology, D.L. (Dengsheng Lu), G.L., D.L. (Dengqiu Li), Q.W. and X.S.; software, D.L. (Dengsheng Lu) and X.S.; validation, D.L. (Dengqiu Li) and X.S.; formal analysis, G.L. and X.S.; investigation, D.L. (Dengqiu Li), Q.W. and X.S.; resources, D.L. (Dengsheng Lu), G.L., D.L. (Dengqiu Li) and Q.W.; data curation, D.L. (Dengqiu Li), Q.W. and X.S.; writing—original draft preparation, X.S., G.L. and D.L. (Dengsheng Lu); writing—review and editing, D.L. (Dengsheng Lu), G.L., D.L. (Dengqiu Li), Q.W. and X.S.; visualization, D.L. (Dengsheng Lu), G.L. and D.L. (Dengqiu Li); supervision, D.L. (Dengsheng Lu) and G.L.; project administration, D.L. (Dengsheng Lu) and D.L. (Dengqiu Li); funding acquisition, D.L. (Dengsheng Lu) and D.L. (Dengqiu Li). All authors have read and agreed to the published version of the manuscript.

**Funding:** This research was funded by Department of Water Resources at Fujian Province, grant numbers MSK202207 and MSK202311, Ministry of Water Resources, grant number SKS-2022083, and Fujian Provincial Science and Technology Department, grant number 2021R1002008.

**Data Availability Statement:** Landsat time series data can be obtained via the GEE platform at <https://earthengine.google.com> (accessed on 1 March 2023). The SRTM DEM data with a resolution of 30 m were downloaded from the USGS website (<https://lpdaac.usgs.gov/> (accessed on 15 November 2022)). Other data sources such as field survey can be obtained from Dengsheng Lu at Fujian Normal University upon request.

**Acknowledgments:** The authors would like to thank Wenlin Yang, Yongpeng Ye, Ming Zhang, Xu Zhang, Aoni Shi, and Ganlin Feng for their help during the field survey.

**Conflicts of Interest:** The authors declare no conflicts of interest. The funders had no role in the design of the study; in the collection, analyses, or interpretation of data; in the writing of the manuscript; or in the decision to publish the results.

## References

- Montgomery, D.R. Soil Erosion and Agricultural Sustainability. *Proc. Natl. Acad. Sci. USA* **2007**, *104*, 13268–13272. [[CrossRef](#)] [[PubMed](#)]
- Gilani, H.; Ahmad, A.; Younes, I.; Abbas, S. Impact Assessment of Land Cover and Land Use Changes on Soil Erosion Changes (2005–2015) in Pakistan. *Land Degrad. Dev.* **2022**, *33*, 204–217. [[CrossRef](#)]
- Crosson, P. Soil Erosion Estimates and Costs. *Science* **1995**, *269*, 461–464. [[CrossRef](#)] [[PubMed](#)]
- Borrelli, P.; Panagos, P.; Alewell, C.; Ballabio, C.; de Oliveira Fagundes, H.; Haregeweyn, N.; Lugato, E.; Maerker, M.; Poesen, J.; Vanmaercke, M.; et al. Policy Implications of Multiple Concurrent Soil Erosion Processes in European Farmland. *Nat. Sustain.* **2023**, *6*, 103–112. [[CrossRef](#)]
- Wuepper, D.; Borrelli, P.; Finger, R. Countries and the Global Rate of Soil Erosion. *Nat. Sustain.* **2020**, *3*, 51–55. [[CrossRef](#)]
- Aneseyee, A.B.; Elias, E.; Soromessa, T.; Feyisa, G.L. Land Use/land Cover Change Effect on Soil Erosion and Sediment Delivery in the Winike Watershed, Omo Gibe Basin, Ethiopia. *Sci. Total Environ.* **2020**, *728*, 138776. [[CrossRef](#)] [[PubMed](#)]
- Ahmad, N.S.B.N.; Mustafa, F.B.; Didams, G. A Systematic Review of Soil Erosion Control Practices on the Agricultural Land in Asia. *Int. Soil Water Conserv. Res.* **2020**, *8*, 103–115. [[CrossRef](#)]
- Senanayake, S.; Pradhan, B. Predicting Soil Erosion Susceptibility Associated with Climate Change Scenarios in the Central Highlands of Sri Lanka. *J. Environ. Manag.* **2022**, *308*, 114589. [[CrossRef](#)]
- Belachew, A.; Mekuria, W.; Nachimuthu, K. Factors Influencing Adoption of Soil and Water Conservation Practices in the Northwest Ethiopian Highlands. *Int. Soil Water Conserv. Res.* **2020**, *8*, 80–89. [[CrossRef](#)]
- Du, X.; Jian, J.; Du, C.; Stewart, R. Conservation Management Decreases Surface Runoff and Soil Erosion. *Int. Soil Water Conserv. Res.* **2021**, *10*, 188–196. [[CrossRef](#)]
- Hua, F.; Bruijnzeel, L.A.; Meli, P.; Martin, P.A.; Zhang, J.; Nakagawa, S.; Miao, X.; Wang, W.; McEvoy, C.; Peña-Arancibia, J.L.; et al. The Biodiversity and Ecosystem Service Contributions and Trade-Offs of Forest Restoration Approaches. *Science* **2022**, *376*, 839–844. [[CrossRef](#)]
- Yang, X.; Jia, Z.; Ci, L. Assessing Effects of Afforestation Projects in China. *Nature* **2010**, *466*, 315. [[CrossRef](#)]
- Gong, W.; Liu, T.; Duan, X.; Sun, Y.; Zhang, Y.; Tong, X.; Qiu, Z. Estimating the Soil Erosion Response to Land-Use Land-Cover Change Using GIS-Based RUSLE and Remote Sensing: A Case Study of Miyun Reservoir, North China. *Water* **2022**, *14*, 742. [[CrossRef](#)]
- Guo, X.; Shao, Q.; Luo, Y. Effects of Different Management Measures on Soil Conservation and the Influence of Environmental Conditions: A Case Study Involving UAV Remote Sensing on the Loess Plateau. *Remote Sens. Ecol. Conserv.* **2022**, *8*, 683–697. [[CrossRef](#)]
- Zhang, X.C.; Nearing, M.A.; Risse, L.M.; McGregor, K.C. Evaluation of WEPP Runoff and Soil Loss Predictions Using Natural Runoff Plot Data. *Trans. ASAE* **1996**, *39*, 855–863. [[CrossRef](#)]
- Mathys, N.; Brochot, S.; Meunier, M.; Richard, D. Erosion Quantification in the Small Marly Experimental Catchments of Draix (Alpes de Haute Provence, France). Calibration of the ETC Rainfall–Runoff–Erosion Model. *Catena* **2003**, *50*, 527–548. [[CrossRef](#)]
- Lu, D.; Li, G.; Valladares, G.; Batistella, M. Mapping Soil Erosion Risk in Rondônia, Brazilian Amazonia: Using RUSLE, Remote Sensing and GIS. *Land Degrad. Dev.* **2004**, *15*, 499–512. [[CrossRef](#)]
- Gao, G.; Liang, Y.; Liu, J.; Dunkerley, D.; Fu, B. A Modified RUSLE Model to Simulate Soil Erosion under Different Ecological Restoration Types in the Loess Hilly Area. *Int. Soil Water Conserv. Res.* **2023**. [[CrossRef](#)]
- Gao, J.; Shi, C.; Yang, J.; Yue, H.; Liu, Y.; Chen, B. Analysis of Spatiotemporal Heterogeneity and Influencing Factors of Soil Erosion in a Typical Erosion Zone of the Southern Red Soil Region, China. *Ecol. Indic.* **2023**, *154*, 110590. [[CrossRef](#)]
- Cheng, Z.; Lu, D.; Li, G.; Huang, J.; Sinha, N.; Zhi, J.; Li, S. A Random Forest–Based Approach to Map Soil Erosion Risk Distribution in Hickory Plantations in Western Zhejiang Province, China. *Remote Sens.* **2018**, *10*, 1899. [[CrossRef](#)]

21. Huang, J.; Lu, D.; Li, J.; Wu, J.; Chen, S.; Zhao, W.; Ge, H.; Huang, X.; Yan, X. Integration of Remote Sensing and GIS for Evaluating Soil Erosion Risk in Northwestern Zhejiang, China. *Photogramm. Eng. Rem. Sens.* **2012**, *78*, 935–946. [CrossRef]
22. Zhou, P.; Luukkanen, O.; Tokola, T.; Nieminen, J. Effect of Vegetation Cover on Soil Erosion in a Mountainous Watershed. *Catena* **2008**, *75*, 319–325. [CrossRef]
23. Shi, P.; Li, P.; Li, Z.; Sun, J.; Wang, D.; Min, Z. Effects of Grass Vegetation Coverage and Position on Runoff and Sediment Yields on the Slope of Loess Plateau, China. *Agric. Water Manag.* **2022**, *259*, 107231. [CrossRef]
24. Wei, S.; Zhang, K.; Liu, C.; Cen, Y.; Xia, J. Effects of Different Vegetation Components on Soil Erosion and Response to Rainfall Intensity under Simulated Rainfall. *Catena* **2024**, *235*, 107652. [CrossRef]
25. Lu, D.; Batistella, M.; Moran, E.; Hetrick, S.; Alves, D.; Brondizio, E. Fractional Forest Cover Mapping in the Brazilian Amazon with a Combination of MODIS and TM images. *Int. J. Remote Sens.* **2011**, *32*, 7131–7149. [CrossRef]
26. Li, D.; Lu, D.; Zhao, Y.; Zhou, M.; Chen, G. Spatial Patterns of Vegetation Change in Giant Panda Habitat Based on MODIS Time-Series Observations and Local Indicators of Spatial Association. *Ecol. Indic.* **2021**, *124*, 107418. [CrossRef]
27. Li, D.; Lu, D.; Li, N.; Wu, M.; Shao, X. Quantifying Annual Land-Cover Change and Vegetation Greenness Variation in A Coastal Ecosystem Using Dense Time-Series Landsat Data. *GISci. Remote Sens.* **2019**, *56*, 769–793. [CrossRef]
28. Yu, X.; Lu, D.; Jiang, X.; Li, G.; Chen, Y.; Li, D.; Chen, E. Examining the Roles of Spectral, Spatial, and Topographic Features in Improving Land-Cover and Forest Classifications in a Subtropical Region. *Remote Sens.* **2020**, *12*, 2907. [CrossRef]
29. Zhu, Z. Change Detection Using Landsat Time Series: A Review of Frequencies, Preprocessing, Algorithms, and Applications. *ISPRS J. Photogramm. Remote Sens.* **2017**, *130*, 370–384. [CrossRef]
30. Zhu, Z.; Zhang, J.; Yang, Z.; Aljaddani, A.; Cohen, W.; Qiu, S.; Zhou, C. Continuous Monitoring of Land Disturbance Based on Landsat Time Series. *Remote Sens. Environ.* **2019**, *238*, 111116. [CrossRef]
31. Legleiter, C.J.; King, T.V.; Carpenter, K.D.; Hall, N.C.; Mumford, A.C.; Slonecker, T.; Graham, J.L.; Stengel, V.G.; Simon, N.; Rosen, B.H. Spectral Mixture Analysis for Surveillance of Harmful Algal Blooms (SMASH): A Field-, Laboratory-, and Satellite-Based Approach to Identifying Cyanobacteria Genera from Remotely Sensed Data. *Remote Sens. Environ.* **2022**, *279*, 113089. [CrossRef]
32. Song, D.; Wang, Z.; He, T.; Wang, H.; Liang, S. Estimation and Validation of 30 M Fractional Vegetation Cover over China through Integrated Use of Landsat 8 and Gaofen 2 Data. *Sci. Remote Sens.* **2022**, *6*, 100058. [CrossRef]
33. Nill, L.; Grünberg, I.; Ullmann, T.; Gessner, M.; Boike, J.; Hostert, P. Arctic Shrub Expansion Revealed by Landsat-Derived Multitemporal Vegetation Cover Fractions in the Western Canadian Arctic. *Remote Sens. Environ.* **2022**, *281*, 113228. [CrossRef]
34. Lu, D.; Moran, E.; Batistella, M. Linear Mixture Model Applied to Amazonian Vegetation Classification. *Remote Sens. Environ.* **2003**, *87*, 456–469. [CrossRef]
35. Lu, D.; Batistella, M.; Mausel, P.; Moran, E. Mapping and Monitoring Land Degradation Risks in the Western Brazilian Amazon Using Multitemporal Landsat TM/ETM+ Images. *Land Degrad. Dev.* **2007**, *18*, 41–54. [CrossRef]
36. Tang, C.; Liu, Y.; Li, Z.; Guo, L.; Xu, A.; Zhao, J. Effectiveness of Vegetation Cover Pattern on Regulating Soil Erosion and Runoff Generation in Red Soil Environment, Southern China. *Ecol. Indic.* **2021**, *129*, 107956. [CrossRef]
37. Kijowska-Strugała, M.; Bucala-Hrabia, A.; Demczuk, P. Long-Term Impact of Land Use Changes on Soil Erosion in an Agricultural Catchment (in the Western Polish Carpathians). *Land Degrad. Dev.* **2018**, *29*, 1871–1884. [CrossRef]
38. Wu, G.; Liu, Y.; Cui, Z.; Liu, Y.; Shi, Z.; Yin, R.; Kardol, P. Trade-off between Vegetation Type, Soil Erosion Control and Surface Water in Global Semi-Arid Regions: A Meta-Analysis. *J. Appl. Ecol.* **2020**, *57*, 875–885. [CrossRef]
39. Cao, S.; Zhong, B.; Yue, H.; Zeng, H.; Zeng, J. Development and Testing of a Sustainable Environmental Restoration Policy on Eradicating the Poverty Trap in China's Changting County. *Proc. Natl. Acad. Sci. USA* **2009**, *106*, 10712–10716. [CrossRef] [PubMed]
40. Wang, C.; Yang, Y.; Zhang, Y. Economic Development, Rural Livelihoods, and Ecological Restoration: Evidence from China. *Ambio J. Hum. Environ.* **2011**, *40*, 78–87. [CrossRef] [PubMed]
41. Yang, X.; Zhong, B.; Xie, X. *Soil Erosion and Conservation in Red-Soil Hill Area*; China Agricultural Press: Beijing, China, 2005.
42. Zeng, J.; Zhong, B. Historical Changes in Strategies to Control Soil and Water Erosion in Changting County. *Fujian Soil Water Conserv.* **2002**, *14*, 37–39.
43. Chen, Z. Desertification Induced by Water Erosion and Its Combat of Hetian Town in Changding County, Fujian province. *Prog. Geogr.* **1998**, *64*, 834–841.
44. Wang, C.; Yang, Y.; Zhang, Y. Rural Household Livelihood Change, Fuel Wood Substitution, and Hilly Ecosystem Restoration: Evidence from China. *Renew. Sustain. Energy Rev.* **2012**, *16*, 2475–2482. [CrossRef]
45. Wang, C.; Yang, Y.; Zhang, Y. Cost-Effective Targeting Soil and Water Conservation: A Case Study of Changting County in Southeast China. *Land Degrad. Dev.* **2015**, *27*, 387–394. [CrossRef]
46. Zeng, C.; Zheng, D. *Research on the Ecological Environment of Typical Areas of Fujian*; China Environmental Science Press (Chinese): Beijing, China, 2006.
47. Beijing Review. The Changting Experience: China's Soil Erosion Prevention and Control. 8 November 2023. Available online: [http://mp42.china.com.cn/video\\_tide/2023/11/7/20231171699356192321\\_376.mp4](http://mp42.china.com.cn/video_tide/2023/11/7/20231171699356192321_376.mp4) (accessed on 15 December 2023).
48. Maiersperger, T.K.; Scaramuzza, P.; Leigh, L.; Shrestha, S.; Gallo, K.; Jenkerson, C.; Dwyer, J. Characterizing LEDAPS Surface Reflectance Products by Comparisons with AERONET, Field Spectrometer, and MODIS Data. *Remote Sens. Environ.* **2013**, *136*, 1–13. [CrossRef]

49. Skakun, S.; Vermote, E.; Roger, J.-C.; Justice, C.; Masek, J. Validation of the LaSRC Cloud Detection Algorithm for Landsat 8 Images. *IEEE J. Sel. Top. Appl. Earth Obs. Remote Sens.* **2019**, *12*, 2439–2446. [[CrossRef](#)]
50. Poortinga, A.; Tenneson, K.; Shapiro, A.; Nguyen, Q.; San Aung, K.; Chishtie, F.; Saah, D. Mapping Plantations in Myanmar by Fusing Landsat-8, Sentinel-2 and Sentinel-1 Data along with Systematic Error Quantification. *Remote Sens.* **2019**, *11*, 831. [[CrossRef](#)]
51. Jiang, X.; Li, G.; Lu, D.; Erxue, C.; Wei, X. Stratification-Based Forest Aboveground Biomass Estimation in a Subtropical Region Using Airborne Lidar Data. *Remote Sens.* **2020**, *12*, 1101. [[CrossRef](#)]
52. Choudhury, B.J.; Ahmed, N.U.; Idso, S.B.; Reginato, R.J.; Daughtry, C.S.T. Relations between Evaporation Coefficients and Vegetation Indices Studied by Model Simulations. *Remote Sens. Environ.* **1994**, *50*, 1–17. [[CrossRef](#)]
53. Montandon, L.; Small, E. The Impact of Soil Reflectance on the Quantification of the Green Vegetation Fraction from NDVI. *Remote Sens. Environ.* **2008**, *112*, 1835–1845. [[CrossRef](#)]
54. Jiapaer, G.; Chen, X.; Bao, A. A Comparison of Methods for Estimating Fractional Vegetation Cover in Arid Regions. *Agric. For. Meteorol.* **2011**, *151*, 1698–1710. [[CrossRef](#)]
55. Moisen, G.; Meyer, M.; Schroeder, T.; Liao, X.; Schleeweis, K.; Freeman, E.; Toney, J. Shape Selection in Landsat Time Series: A Tool for Monitoring Forest Dynamics. *Glob. Chang. Biol.* **2016**, *22*, 3518–3528. [[CrossRef](#)] [[PubMed](#)]
56. Ge, X.G.; Xiao, W.F.; Zeng, L.X.; Huang, Z.L.; Lei, J.P.; Li, M.H. The Link between Litterfall, Substrate Quality, Decomposition Rate, and Soil Nutrient Supply in 30-Year-Old Pinus Massoniana Forests in the Three Gorges Reservoir Area, China. *Soil Sci.* **2013**, *178*, 442–451. [[CrossRef](#)]
57. Wu, X.; Zhu, C.; Yu, J.; Zhai, L.; Zhang, H.; Yang, K.; Hou, X. Ecological Vulnerability in the Red Soil Erosion Area of Changting under Continuous Ecological Restoration: Spatiotemporal Dynamic Evolution and Prediction. *Forests* **2022**, *13*, 2136. [[CrossRef](#)]
58. Guo, T. Environmental and Economic Analysis and Future Strategic Strategies in Changting County, Fujian Province—Based on the History of Soil and Water Loss Control. *Contemp. Econ.* **2011**, *24*, 102–105.
59. Chen, Z.; Yue, H. Analysis of Microclimate Effects after Implementing Soil and Water Conservation Measures: Taking the Hetian Area of Changting as an Example. *Subtrop. Soil Water Conserv.* **2005**, *1*, 17–23.
60. Berendse, F.; van Ruijven, J.; Jongejans, E.; Keesstra, S. Loss of Plant Species Diversity Reduces Soil Erosion Resistance. *Ecosystems* **2015**, *18*, 881–888. [[CrossRef](#)]
61. Zhao, G.; Mu, X.; Wen, Z.; Wang, F.; Gap, P. Soil Erosion, Conservation, and Eco-Environment Changes in the Loess Plateau of China. *Land Degrad. Dev.* **2013**, *24*, 499–510. [[CrossRef](#)]
62. Bai, Y.; Zha, X.; Chen, S. Effects of the Vegetation Restoration Years on Soil Microbial Community Composition and Biomass in Degraded Lands in Changting County, China. *J. For. Res.* **2020**, *31*, 1295–1308. [[CrossRef](#)]
63. Xu, H.; He, H.; Huang, S. Analysis of Fractional Vegetation Cover Change and Its Impact on Thermal Environment in the Hetian Basinal Area of County Changting, Fujian Province, China. *Acta Ecol. Sin.* **2013**, *33*, 2954–2963.
64. Altieri, M.; Nicholls, C. *Biodiversity and Pest Management in Agroecosystems*; CRC Press: Boca Raton, FL, USA, 2004.
65. Xie, J.; Guo, J.; Yang, Z.; Huang, Z.; Chen, G.; Yang, Y. Rapid Accumulation of Carbon on Severely Eroded Red Soils through Afforestation in Subtropical China. *For. Ecol. Manag.* **2013**, *300*, 53–59. [[CrossRef](#)]
66. Chen, Y.; Chen, L.; Cheng, Y.; Ju, W.; Chen, H.Y.H.; Ruan, H. Afforestation Promotes the Enhancement of Forest LAI and NPP in China. *For. Ecol. Manag.* **2020**, *462*, 117990. [[CrossRef](#)]
67. Ghazoul, J.; Chazdon, R. Degradation and Recovery in Changing Forest Landscapes: A Multiscale Conceptual Framework. *Annu. Rev. Environ. Resour.* **2016**, *42*, 161–188. [[CrossRef](#)]
68. Gong, C.; Tan, Q.; Liu, G.; Xu, M. Impacts of Mixed Forests on Controlling Soil Erosion in China. *Catena* **2022**, *213*, 106147. [[CrossRef](#)]
69. Zhang, S.; Zhu, X.; Wang, X. Monitoring Vegetation Restoration in Soil and Water Loss Governance Area in Changting County Based on Interannual Landsat Time-Series Dataset. *J. Yangtze River Sci. Res. Inst.* **2020**, *37*, 43–49.
70. Chen, J.; Xiao, H.; Li, Z.; Liu, C.; Ning, K.; Tang, C. How Effective Are Soil and Water Conservation Measures (SWCMs) in Reducing Soil and Water Losses in the Red Soil Hilly Region of China? A Meta-Analysis of Field Plot Data. *Sci. Total Environ.* **2020**, *735*, 139517. [[CrossRef](#)]

**Disclaimer/Publisher’s Note:** The statements, opinions and data contained in all publications are solely those of the individual author(s) and contributor(s) and not of MDPI and/or the editor(s). MDPI and/or the editor(s) disclaim responsibility for any injury to people or property resulting from any ideas, methods, instructions or products referred to in the content.